Anticipating the Hazard of Glacial Lake Outburst Floods in Karakoram

Nazir Ahmed Bazai [1,2], Paul A. Carling [3*], Peng Cui [2,4*], Hao Wang [2,4], Zhang Guotao [4], Liu Dingzhu [4,5 6], Javed Hassan [7]

[1] Key Laboratory of Mountain Hazards and Earth Surface Process/Institute of Mountain Hazards and Environment, Chinese Academy of Sciences (CAS), Chengdu, China
[2] China-Pakistan Joint Research Center on Earth Sciences, Chinese Academy of Sciences and HEC, Islamabad, Pakistan.
[3] Geography and Environmental Science, University of Southampton, Southampton SO17 1BJ, UK
[4] Institute of Geographic Sciences and Natural Resources Research, Chinese Academy of Sciences, Beijing, China
[5] Earth Surface Process Modelling, German Research Centre for Geosciences (GFZ), Potsdam, Germany
[6] National Disaster Reduction Centre of China, Ministry of Emergency Management, Beijing, China
[7] DTU Space, Technical University of Denmark, 2800 Kongens Lyngby, Denmark

Correspondence to: Paul A. Carling: p.a.carling@soton.ac.uk and Peng Cui: pengcui@imde.ac.cn

Abstract. Climate change leads to changes in glacier mass balance, including steady advancements and surges that reposition the glacier snouts. Glacier advancement can dam proglacial meltwater lakes. Within the Karakoram and surrounding regions, the positive feedback of climate change has resulted in more frequent ice-dammed glacial lake outburst floods (GLOFs), often facilitated by englacial conduits. However, the complex and multi-factor processes of conduit development are difficult to measure. Determining the lake depths that might trigger GLOFs and the numerical model specifications for breaching are challenging. Empirical estimates of lake volumes, along with field-based monitoring of lake levels and depths and the assessment of GLOF hazards, enable warnings and damage mitigation. Using historical data, remote sensing techniques, high-resolution imagery, cross-correlation feature-tracking, and field-based data, we identified the processes of lake formation, drainage timing, and triggering depth. We developed empirical approaches to determine lake volume and trigger water pressure leading to a GLOF. An albeit weak correlation between glacier surge velocity and lake volume reveals that glacier surge velocity may play a crucial role in lake formation and thus controls the size and volume of the lake. Lake volume estimation involves geometric considerations of the lake basin shape. A GLOF becomes likely when the lake's normalized depth (n') exceeds 0.60, equivalent to a typical water pressure on the dam face of 510 kPa. These fields and remotely sensed findings not only offer valuable insights for early warning procedures in the Karakoram but also suggest that similar approaches might be effectively applied to other mountain environments worldwide where GLOFs pose a hazard.

1. Introduction

Globally, glacier shrinkage is a strikingly visible sign of climate change, as is an apparent increase in the number of glacier avalanches (Byers et al., 2023; Kääb and Girod, 2023; Li et al., 2024; You and Xu, 2022) and glacial lake outburst floods (GLOFs) (Bazai et al., 2021; Bhambri et al., 2019; Emmer, 2017; Zheng et al., 2021). However, within High Mountain Asia (HMA), particularly the Karakoram, Kunlun Shan, and Eastern Pamirs, the glaciers gained mass since 1970 (Berthier and

Deleted: Anticipating
Deleted: Risk
Deleted: Climate change leads to changes in glacier mass balance, including steady advancements and surges that reposition the glacier snouts . Glacier advancement can dam proglacial meltwater lakes. Within the Karakoram and surrounding regions, he positive feedback of climate change has resulted in more frequent ice-dammed glacial lake outburst floods Climate change leads to changes in glacier mass balance, including steady advancements and surges that reposition the glacier snouts . Glacier advancement can dam proglacial meltwater lakes. Within the Karakoram and surrounding regions, he positive feedback of climate change has resulted in more frequent ice-dammed glacial lake outburst floods
Deleted: challenging
Deleted: are
Deleted: a challenge
Deleted: risks
Deleted: The
Deleted: of
Deleted: s
Deleted:
Deleted: (Cook & Quincey, 2015)
Deleted: n-dimensional
Deleted: ¶
Deleted: correlating
Deleted: correlating with
Deleted: ..
Deleted: -based
Deleted: empirical
Deleted: can
Formatted: Font color: Black
Commented [PC1]: We have to define terms both in the Abstract and in the main text
Deleted: Globally, glacier shrinkage is a strikingly visible sign of climate change, as is an apparent increase in the number of glacier avalanches
Deleted: .
Deleted: the glaciers gained mass since 1970

Brun, 2019; Gardelle et al., 2012; Kääb et al., 2015; Minora et al., 2013; Yao et al., 2012). This positive response to climate change may now be over (Jackson et al., 2023), with many glaciers more recently displaying stability (Ali et al., 2021) or retreat (Singh et al., 2023). Nonetheless, the mass gain influenced glacier dynamic behaviours, with the Karakoram glaciers thickening, increasing glacier surges (Bazai et al., 2021; Bazai et al., 2022; Mu et al., 2024), and advancing glacier termini throughout the region (Bhambri et al., 2013; Bolch et al., 2017). This behaviour contrasts with neighboring regions with more sustained negative glacier mass budgets, such as the Himalayas, Hindukush, and Tibet (Bazai et al., 2021; Bolch et al., 2011; Frey et al., 2014). In the latter areas, glaciers continue to shrink, thin, and reduce volume, showing no significant glacier advance (Dehecq et al., 2019; Farinotti et al., 2020; Yao et al., 2012). As a result, the increase in moraine lake formation has increased the number of GLOFs in the glacier-retreating regions (Yong et al., 2017). However, in regions where ice mass has increased, glacier advance has prompted the rapid formation of ice-dammed lakes accompanied by sudden releases of meltwater originating from these lakes (Hewitt, 1982; Hewitt, 1998; Hewitt and Liu, 2010; Singh et al., 2023). Although the number and size of GLOFs may decrease with progressive deglacation (Veh et al., 2023), ice-dammed lake floods currently represent the dominant hazard in cryospheric regions (Veh et al., 2022), comprising 70% of GLOFs through recorded history (Carrivick and Tweed, 2016). In contrast, moraine-dammed lakes contribute only 9% (with the remaining 16%, 3%, and 2 % associated with unknown dam types, volcanic activity, and bedrock failure, respectively) (Carrivick and Tweed, 2016). Specific details of the GLOF hazard for HMA have been compiled by Shrestha et al. (2023).

Herein, the focus is upon ice-dammed lakes. The mechanisms and frequency of ice dam GLOFs remain poorly understood, hindering accurate prediction (Bazai et al., 2021; Cook et al., 2016; Harrison et al., 2018; Richardson and Reynolds, 2000). Recent studies have investigated changes in frequency due to climate change (Rick et al., 2023; Veh et al., 2023), and there are regional assessments of flood volume and hazards (Rick et al., 2023). Despite these efforts, understanding the drainage and predicting flood events from ice-dammed lakes remain challenging. Nonetheless, anticipating the risks associated with these events is crucial due to their potential to cause devastating impacts on human lives and livelihoods, ecosystems, infrastructure (*e.g.*, roads, bridges, hydropower systems), river channel stability, and effects on agriculture and fisheries (Carrivick and Tweed, 2016; Cook et al., 2016; Emmer, 2017; John et al., 2000; Neupane et al., 2019; Zhang et al., 2022). GLOFs have been recorded up to 500 km from ice-dammed lakes (Hewitt and Liu, 2010), resulting in hundreds of human fatalities and the other impacts noted above (Carrivick and Tweed, 2016; Cui et al., 2014; Cui et al., 2015; Kreutzmann, 1994; Mason, 1929; Stuart-Smith et al., 2021; Zhang, 1990; Zheng et al., 2021).

Whilst progress has been made to understand the breaching mechanisms of moraine lake outburst floods, triggered by ice or debris falls, strong earthquake shaking, internal piping, or overtopping waves that exceed the shear resistance of the dam (Emmer and Vilímek, 2013; Richardson and Reynolds, 2000), the understanding of the unclear mechanisms of ice dam lake outburst floods remains a challenge (Werder et al., 2010), making prediction using numerical modelling currently impossible. Therefore, there is an urgent need for simplified approaches to GLOF prediction to mitigate downstream impacts.

Deleted: (Jackson et al., 2023)
Deleted: with many glaciers more recently displaying stability
Deleted: (Ali et al., 2024)
Deleted: or retreat
Deleted: (Singh et al., 2024)
Deleted:
Deleted: Nonetheless, the mass gain influenced glacier dynamic ...
Deleted: (Bazai et al., 2021; 2022; Mu et al., 2024)
Deleted: behaviour contrasts to neighbouring regions with mor ...
Deleted:
Deleted: and reducing
Deleted: As a result, the increase in moraine lake formation has
Deleted: However, in regions where ice mass has increased, ...
Deleted: Although the number and size of GLOFs may decreas ...
Deleted: (Veh et al., 2023)
Deleted: ¶
Deleted: ice-dammed lake floods currently represent the domin ...
Deleted: (Veh et al., 2022)
Deleted: comprising 70% of GLOFs. In contrast, moraine- ...
Deleted: Specific details of the GLOF hazard for HMA have be ...
Deleted: Shrestha et al. (2023)
Deleted:
Deleted: glacial lake outburst floods (
Deleted:)
Deleted: still need to be better
Deleted: global
Deleted: and there are global assessments
Deleted: risk
Deleted: Nonetheless, anticipating
Deleted: causing damage up to 120 km from moraine-dammed ...
Deleted: aroun
Deleted: d
Deleted:
Deleted: resulting in
Deleted: e attempts have
Deleted: explore
Deleted: While attempts have been made to explore the
Deleted: complex and
Deleted: complex
Formatted ...

Despite the uncertainty related to the detail of GLOF initiation, sudden glacier advances during surge cycles have a prominent role in the formation of ice-dammed lakes by creating an ice barrier in the valleys, particularly at narrow valley floor sections and at confluences (Bazai et al., 2021; Bhambri et al., 2019), damming rivers (Singh et al., 2023). Glacier surges have resulted in the formation of ice-dammed lakes in the Swiss Alps (Haeberli, 1983), Northern Norway (Xu et al., 2015), Argentinian Patagonia (Vandekerkhove, 2021), Alaska (Trabant et al., 2003), Karakoram, and in the Pamir (Bazai et al., 2021; Hewitt and Liu, 2010) and Tianshan regions (Ng, 2007; Shangguan et al., 2017). Recent studies reveal that the draining processes of ice-dammed lakes potentially involve one or more mechanisms: subglacial breaching, overspill, rapid ice mass instability, and slow deformation of subglacial cavities (Björnsson, 2003; Haemmig et al., 2014; Round et al., 2017). Several attempts have been made to explore the drainage behaviour of ice-dammed lake outburst floods (Hewitt and Liu, 2010). However, due to the remoteness, danger, and inhospitable terrain where such lakes can be found, real-time data are few, and significant gaps remain in our knowledge of these processes.

In the Karakoram, ice-dammed lakes are found in five major valleys, three of which are densely populated and highly vulnerable to unexpected GLOFs. Recent advances in understanding have been made (Bazai et al., 2021) concerning the formation of episodic ice-dammed lakes, which, due to ice mass transfer variations, are linked to the changes in the glacier surface velocity, ice thickness (Singh et al., 2023) and fluctuations in the crevasse density during the surge cycle (Rea and Evans, 2011; Sharp, 1985). Consequently, herein, we explore two main hypotheses: 1) that lake volume is related to glacier velocity, and 2) that there is a critical lake depth associated with ensuing GLOFs (Thoraninsson, 1939). As lake volume can dictate the characteristics of a GLOF, a third secondary hypothesis was addressed: 3) that ice-dammed lakes can exhibit geometries similar to regular geometric shapes, such that in the absence of detailed lake volume data, lake volumes might be estimated from geometric consideration. Despite advancements in knowledge, globally, the techniques for measuring and estimating lake volume (the volume of the lake before an outburst), the critical depth (for GLOF release), and timely prediction of GLOFs remain largely unexplored or unidentified (Round et al., 2017; Shangguan et al., 2016; Steiner et al., 2018). Very limited ice-dammed lake volume data are available. These ice-dam lake volumes were measured either while the lake basin was empty (after a GLOF event) or partially filled and thus shallow (Round et al., 2017; Shangguan et al., 2016; Steiner et al., 2018). Given that their potential full volumes are unknown, the downstream threat from such lakes remains high. To measure the flood volume and flood magnitude for a deep and potentially full lake, the lake volume measurement is recognized as a critical variable that needs to be accurately calculated or at least well-estimated (Bazai et al., 2021; Bazai et al., 2022). An accurate estimate of lake volume will also help explore the timing, triggering depth of the lake, and frequency of ice-dammed lake outburst floods in relation to surge cycles. Timing information can be approximated by correlating glacier velocities and GLOF occurrences (Bazai et al., 2021; Bazai et al., 2022), which should assist in timely hazard assessment. Herein, the primary objective of this study is to enhance predictive capabilities regarding GLOF event timing by refining empirical lake volume estimation and identifying critical depths for future hazard and risk reduction.

Deleted: minor and major

Deleted: (Singh et al., 2023)

Deleted: surges

Deleted: can

Deleted: can result in

Deleted: are the main agents related to

Deleted: one or more mechanisms:

Formatted: Font color: Black

Deleted: events

Deleted: ice thickness

Deleted: (Signh et al., 2023)

Deleted:

Deleted: he main

Deleted: i

Deleted: Consequently, herein we explore the main hypothesis that lake volume is related to glacier velocity. As lake volume can dictate the characteristics of a GLOF, a secondary hypothesis was addressed that ice-dammed lakes can exhibit geometries similar to regular geometric shapes, such that in the absence of detailed lake volume data, lake volumes might be estimated from geometric consideration.

Deleted: these

Deleted: GLOFs

Deleted: and

Deleted: after a GLOF event

Deleted: The

Deleted: those

Deleted: is extremely

Deleted: The current research focus of Bazai and colleagues aims to leverageThe current research focus of Bazai and colleagues aim to leverage historical records, regular field investigations, and remote sensing techiques techniques to develop a comprehensive understanding, which should lead to better prediction of GLOF volumes and timing volumes and timing through modelling dam failure mechanisms.

2. Study Area

The Karakoram Mountain ranges in HMA are known for their complex geology, climatic variability, and denudation processes, including debris flows, mudflows, landslides, rockfalls, avalanches, and GLOFs. As was noted in the preceding section, changes in glacier dynamics, increasing glacier surges, and a trend of increases in GLOF-related disasters characterize this region. These hazards are responsible for substantial economic losses, including the destruction of residences, infrastructure such as roads and bridges, and agricultural areas, as well as blockages of transportation routes like the Karakoram Highway and other expressways (Shrestha et al., 2023).

Glacier surges in the region have been recorded since the 15th century (Bazai et al., 2021). Since the application of remote sensing to the monitoring of the glaciers from 1970 to 2020, an increasing occurrence of glacier surges has been recorded from the 1990s, with some glacier surges being linked to the formation of ice-dammed lakes and subsequent lake outburst floods. Some lakes persist only seasonally, forming in the winter when temperatures are very low and draining slowly in the spring or summer. Other lakes are more persistent (Bhambri et al., 2019; Hewitt and Liu, 2010), and pose the potential for catastrophic outbursts. The most frequent glacier surges and formation of lakes leading to outburst floods in the Karakoram region occur for the Khurdopin, Kyager, and Shishper glaciers. Although the foreland of the Kyager Glacier, situated in the Shaksgam Valley, is uninhabited, GLOFs have caused damage and losses further downstream. Conversely, GLOFs from the Khurdopin and Shishper glaciers, located in the densely populated Hunza area, have resulted in casualties and substantial economic losses. Consequently, these glaciers and their lakes are selected for study. The focus of the broader investigation is to obtain the data necessary to understand the complex behavior of the glaciers and their drainage systems with a view to anticipating when the occurrence of GLOFs is imminent. Thus, there is an urgent need to identify trigger factors for GLOFs to provide downstream warnings in a timely fashion. Better understanding of the complex process behaviours should eventually lead to improved prediction of such events, not only within the Karakoram, but also worldwide.

Deleted: The Karakoram Mountain ranges in HMA are well known for their complex geology, climatic variability and denudation processes, the latter including: debris flows, mudflows, landslides, rockfalls, and avalanches as well as GLOFs. As was noted in the preceeding section, observed changes in glacier dynamics, increasing glacier surges, and a trend of increases in GLOF-related disasters characterize this region. These hazards are responsible for substantial economic losses, including the destruction of residences, infrastructure such as roads and bridges, and agricultural areas, as well as blockages of transportation routes like the Karakoram Highway and other expressways

Deleted: (Shrestha et al., 2023)

Deleted: (Bazai et al., 2021)Since 2000, an increasing occurrence of glacier surges has been recorded, with some glacier surges being linked to the formation of ice-dammed lakes and subsequent lake outburst floods. These lakes, primarily seasonal(Bhambri et al., 2019; Hewitt and Liu, 2010), pose the potential for catastrophic outbursts. The most frequent glacier surges and formation of lakes leading to outburst floods in the Karakoram region originate from the Khurdopin, Kyager, and Shishper glaciers. Although the foreland of the Kyager Glacier, situated in the Shaksgam Valley, is uninhabited, GLOFs have caused damage and losses further downstream. Conversely, GLOFs from the Khurdopin and Shishper glaciers, located in the densely populated Hunza area, have resulted in casualties and substantial economic losses. Consequently, these glaciers and their lakes are selected for study. The focus of the broader investigation is to obtain the data necessary to understand the complex behaviour of the glaciers and their drainage systems with a view to anticipate when the risk of GLOFs is imminent. Thus, there is an urgent need to identify trigger factors for GLOFs to provide downstream warnings in a timely fashion. Better understanding of the complex process behaviours should eventually lead to improved prediction of such events, not only within the Karakoram, but also worldwide. ¶

Deleted: The g

Deleted: has been on its intervals

Deleted: and has always been responsible for catastrophic floods

Deleted: and studying their behavior

Deleted: drain

Deleted: These lakes, primarily seasonal but some of them last for longer time to a year

Deleted: originate from

Deleted: risk

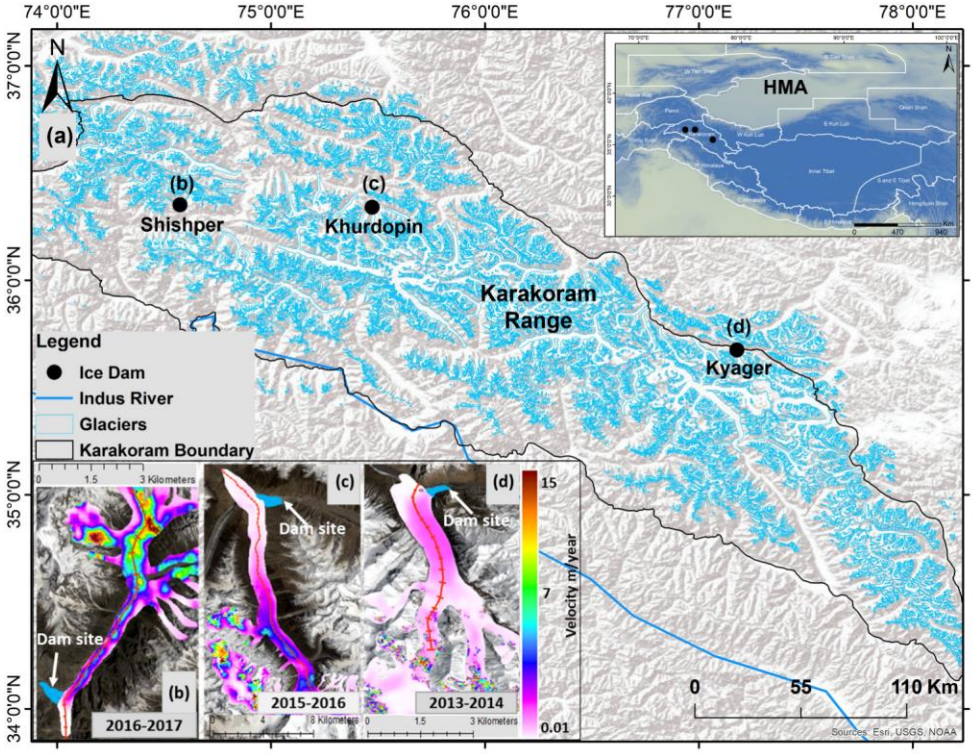

Figure 1: Overview of the study site in the Karakoram (a) and the High Mountain Asia (HMA) region; panels (b-d) present the extent of each glacier at a given time that surge speed has led to ice-dammed lake formation. The associated ice flow velocities are indicated. The background of panels (b-d) are Google Earth© images.

3. Data and Methods:

3.1. Remote sensing data

The identification and mapping of the Khurdopin, Kyager, and Shishper ice-dammed lakes were accomplished using open and commercial satellite imagery sources from 1970 to 2022. The datasets include 590 images of Landsat 2-5, 7-9, and 45 images from Sentinel-2, downloaded from the United States Geological Survey (USGS) website (http://earthexplorer.usgs.gov/) (Table S1). The commercial high-resolution images consisted of 35 images from Gaofen-1 (GF-1) and Gaofen-2 (GF-2), 11

Formatted: Justified

Deleted: comprises, and the source is

Deleted: ©

Deleted:

Deleted: ,Overview of the study site in the Karakoram (a) and the High Mountain Asia (HMA) region; panels (b-d) present the extent of each glacier at a given time that surge speed has led to ice-dammed lake formation. The associated ice flow velocities are indicated. The background of panels (b-d) comprises Google Earth images…

Formatted: Font color: Auto, (Asian) Chinese (China)

Deleted: 3. Data and Methods:¶
3.1. Remote sensing data ¶

Deleted: detection

Deleted: was

images from SPOT-6 and SPOT-7 and five images from Global Planet (https://data.cresda.cn/#/2dMap, https://earth.esa.int/eogateway and https://www.planet.com/products/planet-imagery, respectively). The following DEM datasets have been used to estimate lake volume, depth and dam height: the Advanced Spaceborne Thermal Emission and Reflection Radiometer (ASTER) and the Phased Array type L-band Synthetic Aperture Radar (PALSAR)-DEM data scenes from the National Aeronautics and Space Administration (NASA) Earth Science Data Center website (https://search.earthdata.nasa.gov/). KH-9 and Shuttle Radar Topography Mission (SRTM) data downloaded from http://earthexplorer.usgs.gov/ (Table S2). Field surveys of the Shishper glacier lakes were conducted in 2019, 2021, and 2022 and for Khurdopin in 2017 and 2018 using hand-held GPS and Uncrewed Aerial Vehicles (UAV) (see section 3.2) to determine annual lake extents, lake depths, glacier altitudes, and thickness, termini positions, and glacier surface displacements. The purpose of the field campaigns was to obtain: i) data on processes that could not be derived from remote sensing and; ii) to obtain field data to calibrate/validate remote sensing derived data. The glacier outlines were obtained from the Randolph Glacier Inventory (RGI 6.0) (Consortium, 2017) and modified according to surge movements with time (https://www.planet.com/products/planet-imagery/).

3.2. Glacier lake surface area mapping and glacier surface velocity

Satellite imagery had a spatial resolution of 0.8 to 30 m (Table S1). The use of high-resolution imagery aims to obtain accurate lake surface levels. The images were selected based on the visibility of the glacier surface and lake areas, and overall, 23 ice-dammed lakes from eight surge events were identified related to the Khurdopin, Kyager, and Shishper glaciers (Table 1). The presence of lakes was determined based on the Normalized Difference Water Index (NDWI) (McFeeters, 1996), and the outlines of all 23 lakes were digitized manually using Landsat false-color composites (near-infrared, red, and green bands) to distinguish water bodies from other objects (Huggel et al., 2002). The extent of six Shishper and Khurdopin lakes that occurred after 2017 were obtained in the field using GPS (G639; Accuracy: Single: 1 ~ 3m; SBAS: 0.6m) survey points along the lake shorelines (Fig.2a-d), as well as from Uncrewed Aerial Vehicle (UAV) generated Digital Surface Models (DSMs). Alternatively, high-resolution satellite imagery from Planet (3 m) and GF-1 and 2 (0.8 m to 4 m resolution, respectively) and SPOT-6 and SPOT-7 (1.5 m) were used to extract the lake boundaries. The coupled lake extent and outlines help reduce the uncertainty of the lake extent obtained for Landsat 2-5 images. The above method was used to extract the extent of the previous Khurdopin and Kyager glacier lakes previously reported (Bazai et al., 2021; Bazai et al., 2022), which data are incorporated into the current analysis.

Deleted: estimate

Deleted: were

Deleted:

Deleted: heights

Deleted: For more precise and high-resolution data, field surveys of the Shishper glacier lakes were conducted in 2019, 2021, and 2022 and for Khurdopin in 2017 and 2018 and used Unmanned Aerial Vehicles (UAV) For more precise and high-resolution data, field surveys of the Shishper glacier lakes were conducted in 2019, 2021, and 2022 and for Khurdopin in 2017 and 2018 and used Unmanned Aerial Vehicles (UAV) to determine annual lake extents, lake depths, glacier heights, and thickness, termini positions, and glacier surface displacements. The purpose of the field campagn was to obtain: i) data on processes that could not be derived from remote sensing and; ii) to obtain field data to calibrate/validate remote sensing derived data.The purpose of the field campagn was to obtain: i) data on processes that could not be derived from remote sensing and; ii) to obtain field data to calibrate/validate remote sensing derived data. ¶
The glacier outlines were obtained from the Randolph Glacier Inventory (RGI 6.0) (Consortium, 2017) and modified according to surge movements with time (https://www.planet.com/products/planet-imagery/).¶

Deleted: through optical images

Deleted: manned

Deleted: The use of high-resolution imagery aims to obtain accurate lake surface levels.

Deleted: polygon

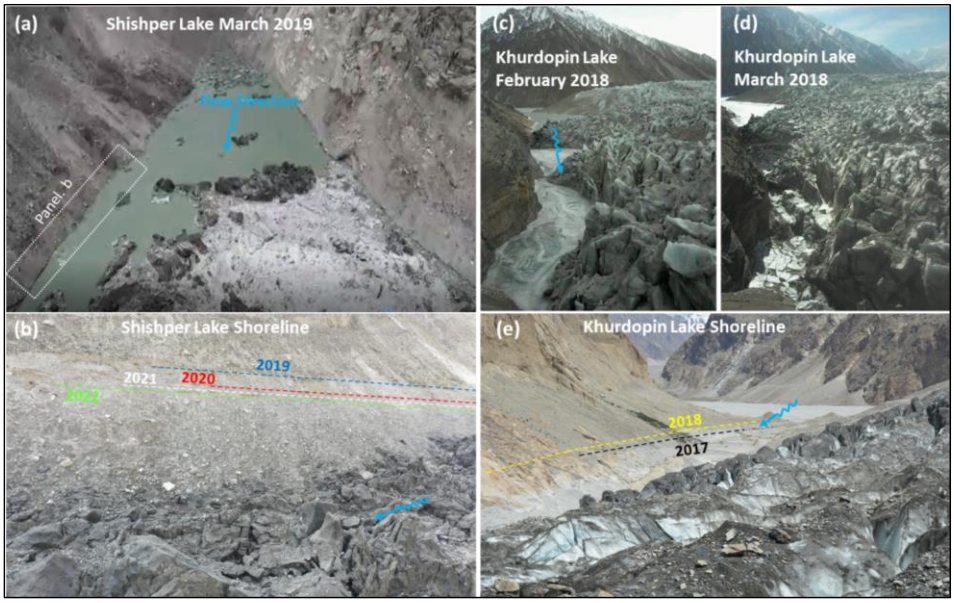

Figure 2: Shishper and Khurdopin glacial lake views in the field. a) Oblique view from a helicopter in March 2019 (image captured during lake monitoring by Gilgit-Baltistan Disaster Management Authority); b) the Shishper shoreline elevations of four lakes that outburst in the given years; c) and d) successive oblique views of the Khurdopin lake in the field; e) Khurdopin lake elevations in the given years. Wiggly blue lines are flow directions.

The Shishper, Khurdopin and Kyager glaciers are surge-type glaciers (Copland et al., 2011; Hewitt, 1998). Since 1972, eight surge events have occurred from Khurdopin (three surges), Kyager (three surges), and Shishper (two surges) (Table 1) at an interval of 17–20 years for each glacier. The Landsat 2-4 images from 1970 to 1990 have errors in the selected glacier area. Therefore, the initial surges for Khurdopin and Kyager between 1970 and 1989 were not considered when estimating the annual velocity. Orthorectified Landsat scenes from TM to OLI–2 and Sentinel 2 were used to estimate the yearly and event-based velocities of all three glaciers from 1989 to 2022 to obtain information about the surge events and glacier front changes. Within this period (1989 to 2022), cloud-free images were chosen each year, although some satellite images were absent. Glacier velocities were recorded as annual averages, although daily measurements of glacier velocity were also determined to assess any effect on lake volume, given the possible velocity sensitivity to the triggering time of GLOFs.

Formatted: Normal

Deleted: in March 2019

Deleted: (Image

Deleted: (GBDMA)

Deleted: the zoom window in panel (a) is presented in panel

Deleted: which

Deleted: are

Deleted: the regular monitoring

Deleted: are the

Deleted: h

Deleted:

Deleted: Shishper and Khurdopin glacial lake view in the field. a) Oblique view from a helicopter in 2019 (image captured in March 2019 during lake monitoring are flow(Image by Gilgit-Baltistan Disaster Management Authority (GBDMA)); the zoom window in panel (a) is presented in panel b) which shows Shishper shoreline elevations of four lakes that outburst in the given years; c and d are the regular monitoring views of the lake in the field; e) are the lake elevations in the given years. Wiggly blue lines areflow directions

Formatted: Font: Bold, Font color: Black

Deleted: The Shishper, Khurdopin and Kyager glaciers are surge-type glaciers (Copland et al., 2011; Hewitt, 1998). Since 1972, eight surge events have occurred from Khurdopin (three surges), Kyager (three surges), and Shishper (two surges) (Table 1) at an interval of 17–20 years for each glaciers. The Landsat 2-4 images from 1970 to 1990 have errors in the selected glacier area. Therefore, the initial surges for Khurdopin and Kyager between 1970 and 1989 were not considered for estimating the annual velocity. Orthorectified Landsat scenes from TM to OLI–2 and Sentinel 2 were used to estimate the yearly and event-based velocities of all three glaciers from 1989 to 2022 to obtain information about the surge events and glacier front changes. Within this period (1989 to 2022), some satellite images were absent, and for precise results, cloud-free images were chosen each year. Glacier velocities were recorded as annual averages, although daily measurements of glacier velocity were also determined to assess note any effect on lake volume, given the likely velocity sensitivity to the triggering time of GLOFs. ¶

Deleted: , and for precise results, cloud-free images were chosen each year

Deleted: also

The surface velocities were extracted along the central line of the Khurdopin, Shishper, and Kyager glaciers, highlighting the quiescent and surge phases obtained from published data (Bazai et al., 2021; Bazai et al., 2022) using image-to-image correlation open-source software COSI-Corr (Leprince et al., 2012; Leprince et al., 2007). The software effectively assesses the glacier surface velocity (Leprince et al., 2012; Steiner et al., 2018). Utilizing a displacement calculation, this technique was used to co-register and correlate surface features (Bazai et al., 2021; Steiner et al., 2018). The surface velocity and overall movement during the surge were measured by observing changes in the GPS-registered glacier front positions every three months from March 2019 and measured for three years for the Shishper glacier in the field as well as for the Khurdopin glacier after six from June 2017 to July 2019. When coupled with COSI-Corr measured velocities, these latter procedures gave accurate results. The velocity estimation procedure generally yields an accuracy of ¼ of a pixel (Sattar et al., 2019). Velocity root-mean-square errors (RMSE) were assessed to justify image processing accuracy. Examples of output are given in Fig. 1b to d.

3.3. Field observation and lake volume measurement

Six lakes were regularly monitored: four from the Shishper Glacier and two from the Khurdopin Glacier. Data for 23 GLOF events from eight surge cycles that occurred during the first year of each surge, or following, are presented in Table 1, with lakes resealing after each GLOF. The field data for six events from the Khurdopin and Shishper glaciers helped to reduce the uncertainty or validated data for 17 lakes for which data were obtained through remote sensing techniques (as explained in section 3.2).

All the previously recorded lakes from Khurdopin and Shishper were drained via single subglacial conduits with stable inlet positions (i.e. the inlet was seen to be in the same place on each occasion) and varying outlet positions and conduit lengths. So, as closely as possible, we identified the inlet and outlet positions of the drainage conduits. As is shown within the Results, the inlet position of the conduit in the ice-dammed lake basin is always in the deepest position. The lowest ice dam height also tended to be in the vicinity of the conduit. The conduit inlet positions were geolocated within the empty lake basins using GPS, and the lake depths were calculated for these locations with reference to shoreline elevations (Table 1 and Figure 2). From the field survey, we noted that the presence of alignments of surface depressions in the glacier indicated the approximate position of curvilinear conduits, from which we estimated the conduit lengths between the inlet and outlet.

Table 1: GLOF and surge date and lake volume measurement since 1970 obtained using remote sensing techniques. The average surge velocity related to each of the 23 GLOFs from eight surge cycles is presented.

Deleted: precise

Formatted: Font color: Auto, English (United Kingdom)

Deleted: The surface velocities extraction along the central line of the Khurdopin, Shishper, and Kyager glaciers are presented in Fig. 1b-d and overall velocity data from 1990 to 2022, highlighting the quiescent and surge phases obtained from published data (Bazai et al., 2021; Bazai et al., 2022) using image-to-image correlation open-source software COSI-Corr (Leprince et al., 2012; Leprince et al., 2007). The software effectively assesses the glacier surface velocity (Leprince et al., 2012; Steiner et al., 2018). Utilizing a displacement calculation, this technique was used to co-register and correlate surface features (Bazai et al., 2021; Steiner et al., 2018). The surface velocity and overall movement during the surge were measured by observing changes in the GPS-registered glacier front positions every three months from March 2019 and measured for three years for the Shishper glacier in the field. When coupled with COSI-Corr measured velocities, these latter procedures gave precise results. The velocity estimation procedure generally yields an accuracy of ¼ of a pixel (Sattar et al., 2019). Velocity root-mean-square errors (RMSE) were assessed to justify the image processing accuracy. ¶

Deleted: validated the data related to 17 lakes obtained through remote sensing techniques noted in section 3.2.

Deleted: All the previously recorded lakes from Khurdopin and Shishper were drained via single subglacial conduits with stable inlet positions and varying outlet positions and conduit lengths. So, as All the previously recorded lakes from Khurdopin and Shishper were drained via single subglacial conduits with stable inlet positions and varying outlet positions and conduit lengths. So, as

Deleted: T

Deleted: the empty lake

Deleted: curvilinear

Deleted:

No.	Glacier Name	Date	Sensor	Lake surface Elevation (m)	Lake Area km^2	Aster/UAV Lake Volume Estimate ($10^6 m^3$)	Lake Vol Uncertainty (+/-$10^6 m^3$)	Vol. after [$10^6 m^3$]	Average velocity (m/d)	Date of next clear image after GLOF	Type of drainage Complete (C) Partial (P)	Surge cycle and Resealed GLOF	Surge Duration in months
	Khurdopin	20/08/1977	LM02									1977–1979	May 1977– Aug 1979; 27 Months
1	Khurdopin	15/8/1999							0.33		C	1998-1999	Jan 1995 to Sep 2002; 92 Months
2	Khurdopin	05/30/2000	L5 TM	3440	1.87	186	2.1	x	0.33	08/26/2000	C	Resealed	
	Khurdopin	04/07/2001	LE07	3416	0.295	19.5	1.5	x	0.44	06/26/2001	C	Resealed	
4	Khurdopin	07/15/2002	LE07	3420	0.60	52.1	1.6	2.2	0.87	08/16/2002	P	Resealed	
5	Khurdopin	07/28/2017	LE07	3415	0.180	16.2	1.4	x	1.41	LC 08 08/01/2017	C	2016-2018	June 2006 to Aug 2009: 38 months
6	Khurdopin	03/18/2018	LC08	3418	0.402	19.8	0.9	x	0.53	02/25/2018	C	Resealed	
7	Kyager	08/01/1977	LM02	4785	1.181	40.73	5.8	x		10/14/1977	C	1976-1977	Jan 1975 to Aug 1978; 43 Months
8	Kyager	07/18/1978	LM02	4810	2.17	82.12	15.6	x		06/07/1979	C	Resealed	
9	Kyager	03/08/1997	L5 TM	4823	3.30	127.3	2.9	x	0.4	04/09/1997	C	1994-1996	Jan 1995 to Sep 2002; 92 Months
10	Kyager	09/10/1998	L5 TM	4825	3.32	133.5	3.5	x	0.3	10/11/1998	C	Resealed	
11	Kyager	09/07/1999	L7ETM+	4813	2.19	86.12	1.23	x	0.46	08/17/1999	C	Resealed	
12	Kyager	06/25/2000	L7ETM+	4778	0.91	23.48	1.12	x	0.49	08/03/2000	C	Resealed	
13	Kyager	09/08/2002	L7ETM+	4819	2.93	115.19	1.09	x	1.29	10/09/2002	C	Resealed	
14	Kyager	06/14/2008	L5 TM	4811	1.45	94.95	1.65	x	0.61	23/06/2008	C	Resealed	June 2006 to Aug 2009: 38 months
15	Kyager	07/28/2009	L5 TM	4808	1.39	91.35	1.56	x	0.56	04/08/2009	C	Resealed	
16	Kyager	07/16/2015	L8 OLI	4800	1.56	53.5	0.87	x	1.14	05/08/2015	C	Resealed	Jan 2013 to Aug 2018: 67 months
17	Kyager	07/14/2016	L7ETM+	4804	1.63	45.89	1.49	2.9	0.53	30/07/2016	P	2014-2016	
18	Kyager	07/31/2016	L7ETM+	4806	1.48	44.32	1.23	x	0.38	08/09/2016	C	Resealed	
19	Kyager	08/10/2017	L8 OLI	4815	2.91	113.99	0.73	11.9	0.38	26/08/2017	P	Resealed	
20	Kyager	08/06/2018	L8 OLI	4807	2.38	87.98	0.53	x	0.29	08/29/2018	C	Resealed	

21	Shishper	06/23/2019	L8 OLI	2650	0.37	24.10	2.1	x	0.95	07/13/2019	C	2017-2019	Dec 2018 to June 2022: 41 Months
22	Shishper	05/29/2020	L8 OLI	2636	0.50	24.90	1.5	x	0.46	06/22/2020	C	Resealed	
23	Shishper	05/16/2021	L8 OLI	2638	0.52	25.77	1.4	x	0.29	07/15/2021	C	Resealed	
	Shishper	05/07/2022	L8 OLI	2641	0.41	27.66	1.1	x	0.24	05/10/2022	C	Resealed	

In addition, we used a UAV (DJI Mavic 2 Pro) equipped with a high-resolution camera (4000 pixels × 2250 pixels) to obtain multiple aerial photographs with a minimum of 85% image overlap (Entwistle and Heritage, 2017; Entwistle and Heritage, 2019; Tonkin and Midgley, 2016). The UAV flew at a low uniform height (500 m - to reduce the image distortion) to generate high-resolution orthomosaics and DSMs of the glacier lake surfaces, empty lake basins, and glacier termini. In addition to UAV data, we utilized data from KH-9 (1974), ASTER (2000-2019), PALSAR-DEM (June 2008), and SRTM (February 2000) for the computation of lake volumes (Table S2). The SRTM DEM without voids serves as the reference dataset, and the vertical uncertainties of the SRTM DEM are reported to be ±10 m (Rodriguez et al., 2006). The corrected DEMs from the Karakoram region are those used by Bazai et al. (2021) and Gardelle et al. (2013).

3.4. Geometry of lake basin

Although in this study, we have field-derived estimates of lake depth, basin geometry, and lake surface area to calculate lake volumes, in many other applications, only remote sensing data are available for undrained lakes. Consequently, considering that the lake area in satellite images often exhibits a triangular planform (*e.g.*, Fig 2a; 3a), we explored the possibility of using a geometric shape to approximate the volume of undrained lake basins. Such an approach would be valuable where the depths of lakes are unknown. To this end, we employ NDWI (as in section 3.1) to identify lake outlines through Landsat false-color composites, which use near-infrared, red, and green bands to distinguish water bodies from other features. We employ standard connected component analysis (Dillencourt et al., 1992) to manually calculate each lake's area, perimeter, and other surface dimensions (as given in Fig. 3b). Initial calculations are pixel-based and later converted to metric units by multiplying pixel counts with their respective pixel sizes. The pixel size for high-resolution images varied from 0.8 to 3 m. The output was cross-validated with Khurdopin and Shishper glacier lakes UAV data having a pixel size of 0.063 m and with field survey evidence. Trials demonstrated that the known volume of the lakes determined using DEMs of the lake basins once drained (section 3.3) could be approximated if the length of the lake from the upstream inlet to the ice-dam face (Z) and the breadth of the lake at the ice dam (C) are known. Given the reported image resolution, uncertainties in the characteristic length measurements (Fig. 3b), measured using GIS 3D interpolation, would translate to uncertainty in lake volume estimates of only 3% when applying Equations 1 and 2 if lake depth was known exactly. For undrained lakes, assuming the depth is the same as the width of the lake at the dam face (Fig. 3b) likely over-estimates lake volume. It might be expected that geometric estimates based on lake surface area alone would be improved if the lake's depth (h) is known at the deepest point close to the dam face. However, in our examples, there is uncertainty in the values of h obtained from DEMs of the drained basins, such that the errors in lake

Deleted: Section Break (Next Page)

Deleted: In addition to UAV data, we utilized data from KH-9 (1974), ASTER (2000-2019), PALSAR-DEM (June 2008), and SRTM (February 2000) for the computation of lake volumes (Table S2). The SRTM DEM without voids serves as the reference dataset, and the vertical uncertainties of the SRTM DEM are reported to be ±10 m

Deleted: The corrected DEMs from the Karakoram region are those used by

Deleted: we have field-derived estimates of lake depth, basin geometry and lake surface area to calculate lake volumes, in many other applications

Deleted: We employ standard connected component analysis

Deleted: to manually calculate each lake's area, perimeter, and other surface dimensions

Deleted: and was

Deleted: It was

Deleted: , as well as

Deleted: uncertainty when applying Equations 1 and 2.

Deleted: sSuch

Deleted: are

Deleted:

Deleted: I

Deleted: is

Deleted: can be

Deleted: a

Deleted: for which

depth estimates translate to errors in lake volume estimates of <14%. Alternatively, where a lake is present, this latter parameter can be obtained by plumbing the depth from a boat.

Given the triangular shape of the lake surface areas, the first consideration with regard to lake geometry was whether the valley sides might be considered to provide a V-shaped lake cross-section or a rectangular cross-section (Fig. 3b), in either case, regular geometric shapes might provide an estimate of the lake volumes. A rectangular cross-section would be closer to the U-shaped valley cross-sections commonly associated with glaciated valleys. Thus, assuming a V-shaped valley, approximating lake volume (V) can be approximated by an irregular tetrahedron (Fig. 3b left-hand panel) where the depth (h) is unknown, but the distance from A to B (X in Fig. 3b) and the length C are known values. Assuming the lake surface is an isosceles triangle, and the vertical face at the dam wall is an equilateral triangle, the volume can be obtained from:

$$V = \sqrt{V^2} \qquad (1)$$

$$V^2 = \frac{1}{144}\left[Y_1^2\, D^2(Z_2^2 + X^2 + C^2 + E^2 - Y_1^2 - D^2) + Y_2^2\, E^2\,(Y_1^2 + X^2 + C^2 + D^2 - Y - E^2)\right.$$
$$\left. + Z^2\, C^2\,(Y_1^2 + Y + D^2 + E^2 - Z^2 - C^2) - Y_1^2 Y_2^2\, C^2 - Y_2^2\, Z^2 D^2 - Y_1^2 Z^2 E^2 - C^2 D^2 E^2\right]$$

where the values for lakeside lengths Y_1 and Y_2, the main length Z, lakeside length D, and lakeside length E are defined in Fig. 3b and obtained from geometry.

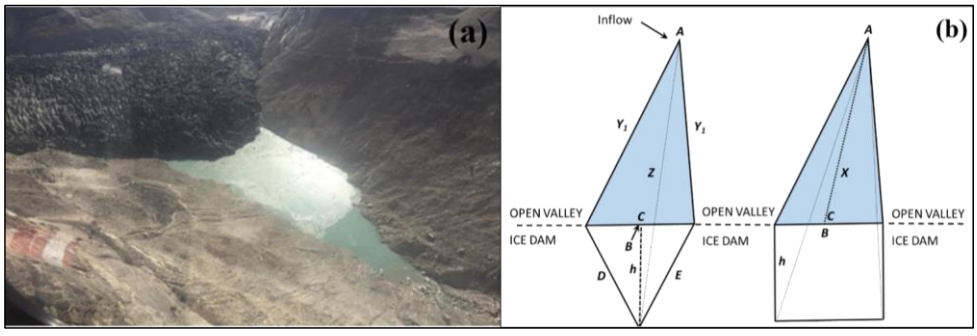

Figure 3: (a) Example of Shishper glacial-dammed lake exhibiting roughly triangular surface 2D shape (see also Fig. 2a); (b) Definition diagram for calculating the volume of the lakes assuming (left) an irregular tetrahedral shape and (right) an irregular pentahedral shape. The blue shading represents the horizontal surface of the lake, and the white area represents the vertical ice wall.

Alternatively, considering a pentahedral, the volume is:

$$V = \tfrac{1}{3}\,(h^2)X. \qquad (2)$$

Deleted: s

Deleted: In our examples this value can be obtained from a DEM of the drained basin, for which the error in lake depth translates to errors in lake volume estimates of <14%.

Deleted: which

Deleted:

Deleted:

Deleted: Thus, assuing a V-shaped valley,

Deleted: approximating

Deleted:

Formatted: Font color: Auto, (Asian) Chinese (China)

Deleted: Alternatively, considering an oblique pentahedral, the volume is:¶
Alternatively, considering an oblique pentahedral, the volume is

Deleted: n

These shape assumptions are addressed within the Discussion.

4. Results

4.1 Surge velocity and ice dam volume

Figure 4a-c presents the relationship between the glacier surge velocity (Khurdopin, Kyager, and Shishper) and 23 GLOFs. The relationship between surge and GLOF was developed using annual average velocity data. The glacier's daily velocity was recorded on the day the GLOF was initiated, as detailed in Table 1. In panels a to c, the GLOF occurred after the peak of the glacier surge, and the resealed lake formed while the surge velocity declined. These responses to slowing the glacier velocity lasted 2-4 years after the surge peak. Thus, GLOFs occur towards the end of a surge period or immediately afterward; the detail is presented in Table 1. The relationship between the timing of glacier surges and the timing of GLOFs is shown in Fig. 4d, wherein the dates of the GLOFs are given as the month in the year. The three Karakoram glaciers can be used as regional examples of surge behavior controlling GLOF occurrence, as there is a temporal relationship between the occurrence of periods of glacier surging and the occurrence of GLOFs (Fig. 4a-d). This pattern of behaviour prompted the hypothesis that glacier thickening and thinning during surging might control the development of ice-dammed lakes (Bazai et al., 2022). Lake volumes would increase when the speed of the ice was low, such that the ice mass would be conserved or increased, and the fracturing of the ice would be reduced. The corollary pertains to when the ice speed increases, the glacier thins, and the fracturing of the ice mass increases, providing hydraulic drainage conduits (Gao et al., 2024). This sequence of events is shown schematically within Fig. 5. A thinning glacier also minimizes potential lake depth and might increase the likelihood of a GLOF occurring over the top of the ice dam.

Deleted: These shape assumptions are addressed within the Discussion

Deleted: The relationship between the glacier surge velocity (Khurdopin, Kyager, and Shishper) and 23 GLOFs is presented in Figure 4a-c wherein the relationship between surge and GLOF was developed using annual average velocity data. The glacier's daily velocity specifically was recorded on the day when the GLOF was initiated, as detailed in Table 1.wherein the relationship between surge and GLOF was developed using annual average velocity data. The glacier's daily velocity specifically was recorded on the day when

Deleted: the GLOF was initiated, as detailed in Table 1.¶

Deleted: of

Deleted: Thus, GLOFs occur towards the end of a surge period or immediately afterward; the detail is presented in Table 1.

Deleted: wherein the dates of the GLOFs are given as the month in the year.

Deleted: regional examples

Deleted: such that ice mass would be conserved or increased, and fracturing of the ice would reduce

Deleted: (Gao *et al*., 2024b)

Deleted: might

Deleted: the

Deleted: ¶

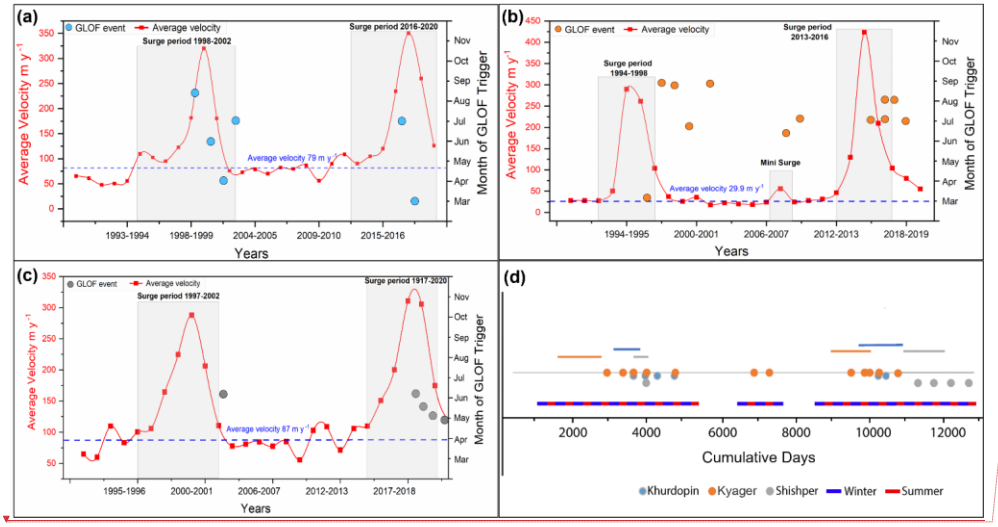

Figure 4: Relationship between glacier surges and GLOFs, with average annual glacier velocity during the surge and quiescent phases for three glaciers: (a) Khurdopin, (b) Kyager, and (c) Shishper. GLOFs for these glaciers occurred between the months of March to November. The combined analysis is presented in (d), illustrating the occurrences of GLOFs (dots) and related periods of glacier surging (bars) as cumulative days since 1st January 1990. Some points are plotted below the timeline to avoid coincident positions. The blue and red lines show the winter (from October to April) and summer (May to September) seasons, with the GLOFs occurring dominantly in the summer months. Within panels a to c, the average surge velocity is given as the red curves, and the average velocity during the study period is given in blue text.

As a first attempt to relate glacier behaviour in a predictive sense to lake formation, we sought to determine the relationship between the resulting lake volume from the prior surge speed. Lake volume should be high when the glacier velocity is low, and the ice mass thickens and *vice versa*; there is some support for this ascertion (Fig. 6). Within Fig. 6, considering all the data (excluding the three drained lakes), the broad data spread prevents the fitting of a significant least-squares regression function. Nonetheless, trial curve fitting showed that a negative power function would be the best fit.

If the volume of a lake decreases as the glacier surge speed increases, as a negative power function would imply, both the lake depth and surface area decrease; then, from an analogy with a pentahedron, the volume of a pentahedron reduces as the square of the characteristic length (Equation 2), here the water depth. Consequently, assuming the pentahedral analogy applies, a least-squares trendline fitting procedure was used to define the constant, α in the function: $V_{DEM} = \alpha U_s^{-2}$ fitted to all the data excluding the drained volumes. This equation, with α = 13.6, is shown in Fig. 6 and visually is a good fit through data for a range of low values of U_s when lake depths will be greatest. Given the data dispersion and the small sample number, there are no statistical outliers (defined objectively; (Carling et al., 2022). An eye-fitted power function has been added to Fig. 6 to tentatively define the lower limit of the data spread.

Deleted:

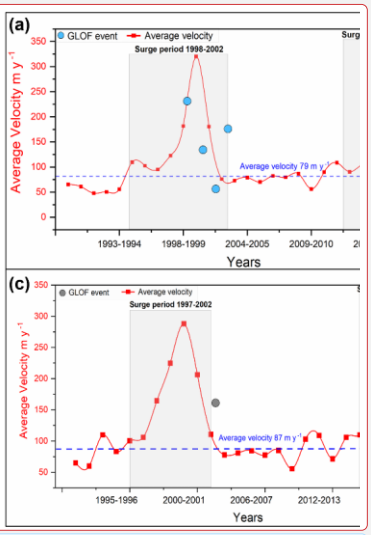

Commented [2]: Fig. 4 is inserted twice here! Which one is the correct version?

Deleted: Relationship between glacier surges and GLOFs, with average annual glacier velocity during the surge and quiescent phases for three glaciers: (a) Khurdopin, (b) Kyager, and (c) ...

Deleted: in

Deleted: text

Deleted: relationship between

Deleted: .

Deleted: 5

Deleted: 5

Deleted: the best fit would be a negative power function

Deleted: ,

Deleted: as a negative power function wouldimply

Deleted: , then

Deleted: (Equation 2)

Deleted: here

Deleted: (If the analogy was with a regular tetrahedron, the lake volume would decrease as a cubic function of the lake depth)

Deleted:

Deleted: 5

Deleted: 5

Deleted: define the lower limit of the data spread tentatively

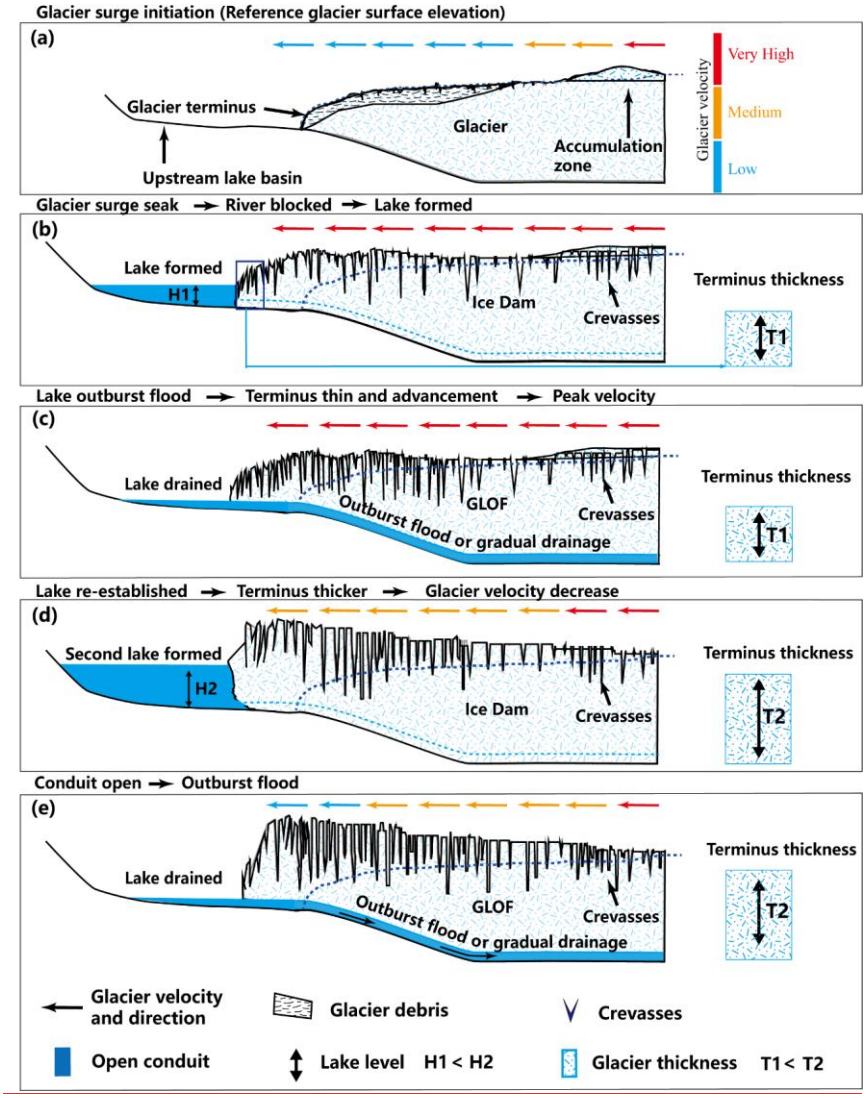
Glacier surge initiation (Reference glacier surface elevation)
(a)
Glacier terminus
Upstream lake basin
Glacier
Accumulation zone
Glacier velocity
Very High
Medium
Low
Glacier surge seak → River blocked → Lake formed
(b)
Lake formed
H1
Ice Dam
Crevasses
Terminus thickness
T1
Lake outburst flood → Terminus thin and advancement → Peak velocity
(c)
Lake drained
GLOF
Crevasses
Outburst flood or gradual drainage
Terminus thickness
T1
Lake re-established → Terminus thicker → Glacier velocity decrease
(d)
Second lake formed
H2
Ice Dam
Crevasses
Terminus thickness
T2
Conduit open → Outburst flood
(e)
Lake drained
GLOF
Crevasses
Outburst flood or gradual drainage
Terminus thickness
T2
Glacier velocity and direction
Glacier debris
Crevasses
Open conduit
Lake level H1 < H2
Glacier thickness T1< T2

685

Figure 5: The mechanism of glacier surge controls lake formation: a) Prior to the surge, there is no stream blockage in front of a thick terminus; b) in the first year of the surge, stream blockage occurs, leading to lake formation behind a thinning terminus; c) during the first year, peak glacier velocity is reached, the lake drains and the terminus thins; d) as surge velocity decreases the lake reforms and the terminus thickens; e) the second lake can drain as velocity continues to decrease and the terminus thickens.

These results, although clearly not definitive, indicate that there likely is a relationship between the volume of the lake and the control of the lake water level exerted by the surge speed. Therefore, surge speed should exert some control on lake depth, volume, and potential GLOF volumes.

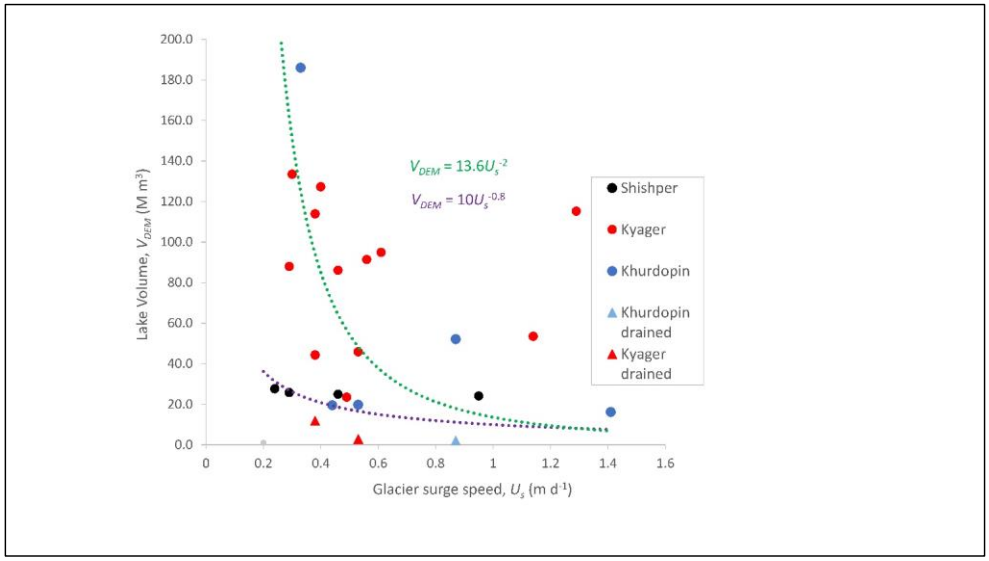

Figure 6: Variation in glacial lake volume as a function of the glacier surge speed. Data from three glaciers. Most lakes drained completely, but three drained lakes had residual volumes (triangles). A -0.8-power function (purple curve) defines the lower limit to the data spread, while a -2.0-power least-squares function (green curve) defines the central tendency of the data trend (see text for explanation).

Given the scatter in the data within Fig. 6, additional data would be required to determine if the relationship between surge speed and lake volume does follows a negative power trend, as we have suggested.

4.2 Tetrahedron assumption for lake volume

Using Equation 1 and assuming the ice dam face was an equilateral triangle, only the values *X* and *C* are required such that the volume of the 'tetrahedron' lakes was around 10 times greater than the volume of the lakes determined using the DEMs (Fig. 7a). This result indicates that the actual depth of the lake (*h*) must be much less than that value associated with an equilateral

Formatted: Font: Bold
Formatted: Font: (Default) Times New Roman, (Asian) Times New Roman, 10 pt, Font color: Text 1, English (United Kingdom)
Formatted: Line spacing: single
Formatted: Font: (Default) Times New Roman, 10 pt
Formatted: Font: (Asian) Times New Roman, Font color: Text 1, English (United Kingdom)
Formatted: Font: (Default) Times New Roman, (Asian) Times New Roman, 10 pt, Font color: Text 1, English (United Kingdom)
Formatted: Font: (Asian) Times New Roman, Font color: Text 1, English (United Kingdom)
Formatted: Font: (Default) Times New Roman, (Asian) Times New Roman, 10 pt, Font color: Text 1, English (United Kingdom)
Formatted: Font: (Asian) Times New Roman, Font color: Text 1, English (United Kingdom)
Formatted: Font: (Default) Times New Roman, (Asian) Times New Roman, 10 pt, Font color: Text 1, English (United Kingdom)
Deleted: likely
Deleted: exert som
Deleted: 5
Deleted:
Deleted: least-squares
Deleted: 5
Deleted:
Deleted: .
Deleted:
Deleted: However, some justification can be provided at this juncture.
Deleted: ***4.2 Tetrahedron assumption for lake volume*** ¶
In passing, it can be noted that the volumes of the irregular tetrahedrons in most cases were not dissimilar to the volumes of regular tetrahedrons (*i.e.*, triangular-based pyramids), the equation for which is simple, in contrast to Equation 1. Nevertheless, using Equation 1, and assuming the ice dam face was an equilateral triangle, only the values *X* and *C* are required such that the volume of the 'tetrahedron' lakes was around 10 times greater than the volume of the lakes determined using the DEMs (Fig. 6a). This result indicates that the actual depth of the lake (*h*) must be much less than that value associated with an equilateral triangle of side length C (Fig. 3b left-hand side). Nevertheless, this procedure provides a means to estimate lake volume from plan-view data alone. ¶ ...
Deleted: In passing, it can be noted that the volumes of the irregular tetrahedrons in most cases were not dissimilar to the ...
Deleted: u

triangle of side length C (Fig. 3b left-hand side). Nevertheless, this procedure provides a means to estimate lake volume from plan-view data alone.

In contrast to the assumption of an equilateral triangle at the dam face, improved lake volume estimates were obtained considering the measured DEM-derived values of h along with the values of X and C. Once again, assuming an irregular tetrahedron as in Fig. 3b, the analysis demonstrated that the tetrahedral lake volume was roughly half that of the DEM volume (not illustrated). This latter result suggests that treating the valley-cross section to be U-shaped (roughly quadrilateral) rather than V-shaped means that doubling the area of the triangular dam face section to form a quadrilateral should provide lake volume estimates, defined as an irregular pentahedron (square-based pyramid) (Fig. 3b right-hand side) closer to the DEM-derived volume estimates.

4.3 Pentahedron assumption for lake volume

The pentahedral volume estimates (Eq. 2), as shown in Fig. 7b, are preferable to those values shown in Fig. 7a. They result in a near 1:1 relationship between V_{Pen} and V_{DEM} but require knowledge of the parameter depth: h, as well as X, and C. If assuming a rectangular base to the pentahedron provided an exact match to the DEM volume, the correlation coefficient value would be unity. Thus, the coefficient of 0.8986 reflects the deviation of the cross-sectional shape of the lake at the dam face from a rectangle. Note that the relationships between both determinations of lake volume (Fig. 7a and b) progressively deviate from a 1:1 relationship as lake volume increases. This trend might indicate that larger lakes are less well-defined as tetrahedrons or pentahedrons as the volumes increase.

Assuming a tetrahedral shape to a lake, then the lake volume can be estimated from remote sensing images alone as only the length of the lake (X) and the breadth of the lake (C) at the ice dam are needed to estimate the lake volume. Assuming a pentahedral shape, the depth (h) of the lake at the ice dam is required as well. Although subsequent to GLOF drainage, h can be measured from a DEM or field survey, for the purposes of mitigation, a warning prior to a GLOF occurring is preferable.

Deleted: ¶

Deleted: improved lake

Deleted: latter

Deleted: ¶

4.3 Pentahedron assumption for lake volume ¶

The pentahedral volume estimates (Eq. 2) as shown in Fig. 6b are preferable to those values shown in Fig. 6b they result in a near 1:1 relationship between V_{Pen} and V_{DEM} but require knowledge of the parameter depth: h, as well as X, and C. If assuming a rectangular base to the pentahedron provided and exact match to the DEM volume, the correlation coefficient value would be unity. Thus, the coefficient of 0.8986 reflects the deviation of the cross-sectional shape of the lake at the dam face from a rectangle. Note that the relationships between both determinations of lake volume (Fig. 6 a and b) progressively deviate from a 1:1 relationship as lake volume increases. This trend might indicate that larger lakes are less well-defined as tetrahedrons or pentahedrons as the volumes increase.¶

Deleted: ¶

Deleted: and so

Deleted: So the depth h could be obtained by deploying a plumb-line or echo-sounder in the lake or estimated through a topographic survey of the bounding slopes.

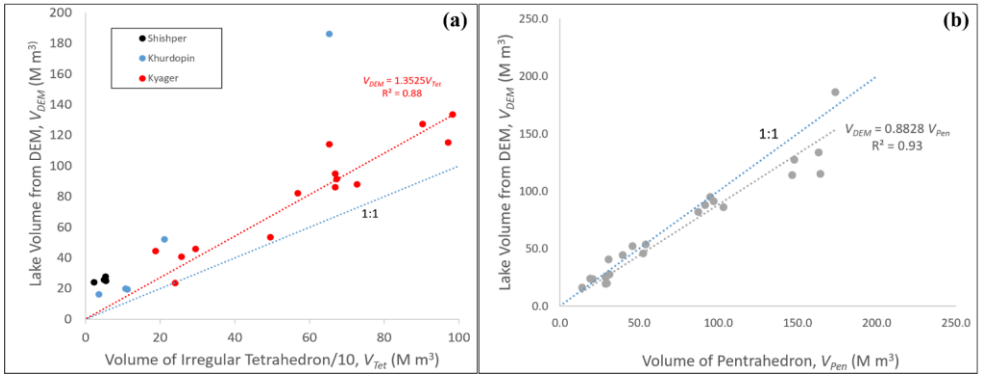

Figure 7: Panel (a) Relationship between the volumes of irregular tetrahedrons/10, derived from Eq. 1, and the volumes of the lakes determined using DEMs. Panel (b) The relationship between the volumes of irregular pentahedrons and the volumes of the lakes was determined using DEMs.

4.4. Anticipating the Timing of GLOF Events

The timing of a GLOF remains difficult to determine, but for tunnel drainage, the main driver is the critical depth. The critical depth is the depth that exerts sufficient pressure at the ice dam wall to induce completed connectivity within the sub-glacial GLOF drainage conduit. For the cases of Shishper, Khurdopin, and Kyager, the glacial lake depths (h) have been normalized by dividing by the minimum value of the ice dam height to give values (n'), normalized lake depths that range between 0 for a fully-drained lake to a hypothetic value of 1 if the lake level reached the height of the ice barrier. At the approximate time of GLOF occurrence, the resulting values of n' range between 0.32 and 0.95 (Fig. 8a-c). Most GLOFs occur for a range of n' values between 0.61 and 0.95 (Fig. 8d). Thus, n' = 0.60 can be regarded as a warning level value with the potential for a GLOF occurring imminently increasing as n' approaches unity.

As the water pressure (P) at the dam face increases linearly with water depth in each lake, any variation in the pressure with n' that deviates from the linear trend reflects changes in the height of the ice dam (Fig. 8d). Thus, for example, the values of pressure for the Shishper lakes around an n' value of 0.8 reflect greater overall deeper and higher ice dam heights in contrast to the Kyager lakes for similar values of n'. The two values of low pressure for n' < 0.6 are associated with relatively low ice dams, and consequently reflect presumed low structural integrity within the ice mass, allowing ready conduit development. Low values of n' (< 0.6) likely are associated with shallow lakes of low hazard potential. Overall, the Kyager data (Fig. 8d) indicate that a minimum water pressure of around 500 kPa should be regarded as a threshold for general concern for GLOF occurrence in the region.

Deleted: 6
Deleted: R
Deleted: Anticipating
Deleted: ,
Deleted: for tunnel draina
Deleted: normalized lake depths,
Deleted: 7a
Deleted: 7d
Deleted: risk of
Deleted: 7d
Deleted: The two values of low pressure for n' < 0.6 reflect low ice dam heights and presumably low structural integrity within the ice mass, allowing ready conduit development.
Deleted: 7d
Formatted: Font color: Auto, (Asian) Chinese (China)

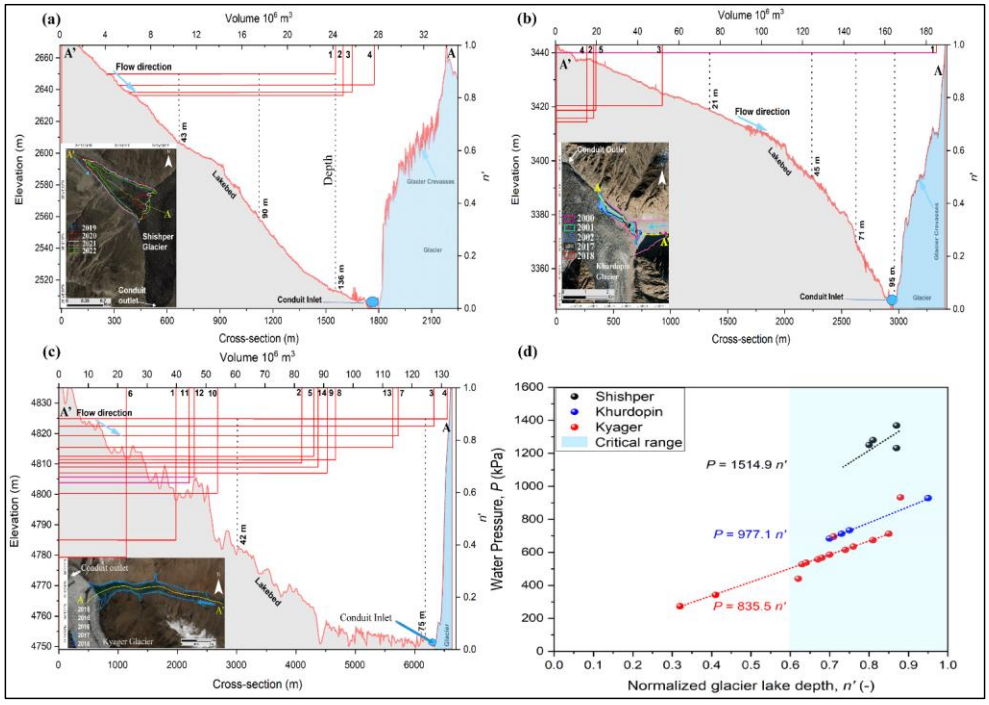

845

Figure 08: The relationship between lake volume and elevation and the critical normalized lake depths for GLOFs. a) Shishper; b) Khurdopin; c) Kyager, redlines connect the relevant elevation and volume in each instance; d) Water pressure at dam face as a function of $n^{'}$. The cross sections are denoted by (A' and A). The date of each lake flood event is shown in Table 1. The straight, solid red lines relate specific lake elevations to volumes. An UAV photograph captured in the field was used for panel a, the images captured by the GF-2 were used for panel b, and Landsat OLI 8 was used for panel c.

850

5. Discussion

Although predictive models related to ice-dam lake development and subsequent GLOF hazard, would best be based on modelling the physics of the systems, the controlling parameters are numerous and complex. For example, the mechanisms of glacial sliding, over-burden pressure, tensile and driving stresses require consideration, as do flexure and ice fracture mechanics, thermal erosion, and water pressure, amongst other controls (Carrivick et al., 2020; Joseph et al., 1996) along with climatic influences (Ng, 2007; Richardson and Reynolds, 2000). Few of these controls are well-understood, and, importantly, even where there is an adequate theory, the field data required to inform modelling are absent for specific potential GLOF locations. In this study, the glacier and lake interactions and their empirical relationships have been explored, and their effect

855

Deleted: 07

Deleted: The relationship between lake volume and elevation and the critical normalized lake depths for GLOFs. a) Shishper; b) Khurdopin; c) Kyager, redlines connect the relevant elevation and volume in each instance; d) Water pressure at dam face as a function of $n^{'}$. The cross sections are denoted by (A' and A). The date of each lake flood event is shown in Table 1. The straight, solid red lines relate specific lake elevations to volumes. A UAV photograph captured in the field were used for panel a, the images captured by the GF-2 were used for panel b, and Landsat OLI 8 was used for panel c

Deleted: risk

Deleted: For example, the mechanisms of glacial sliding, over-burden pressure, tensile and driving stresses require consideration, as do flexure and ice fracture mechanics, thermal erosion, and water pressure, amongst other controls (Carrivick et al., 2020; Joseph et al., 1996) and also climatic influences (Ng, 2007; Richardson and Reynolds, 2000).

Deleted: and also

on lake volume and draining processes examined. Understanding glacier surges, lake formation, and the interactions between lakes and glaciers is crucial for advancing knowledge and developing empirical or numerical GLOF models in mountainous regions (Carrivick et al., 2020; Quincey and Luckman, 2014). Glacier surge speed is routinely determined using remote-sensing imagery (Paul, 2015), as is lake surface area (Quincey and Luckman, 2014). Thus, remote sensing provides a means to develop images similar to Fig. 6 for specific locations around the globe where ice-dammed lakes form due to glacier surging. Although the data within Fig. 6 are scattered, a negative relationship between surge velocity and lake volume is strongly implied. Specifically, data points scatter around a median trend according to a theoretical -2 power function (Fig. 6). Clearly, more data points within Fig. 6 would be desirable such that the relationship (if any) between ice surge velocity and lake volume might be better defined.

There is an urgent need for simpler methods to predict the probable triggering water levels that lead to GLOFs and the likely volume of the ice-dammed lakes that translate into GLOF hydrographs. Given that requirement, it is acknowledged that the relationships proposed herein are empirical and apply specifically to glaciers within the Karakoram region. However, there is no reason to suppose that similar functions based on geometric considerations (Zhang et al., 2023) and a critical depth (Zhao et al., 2017) might not be developed elsewhere, including for moraine-dammed lakes (Yao et al., 2010). Below, the approach is explored for glacial ice-dammed lakes worldwide.

Deleted: Consequently, t

Deleted: here is an urgent need for simpler methods to predict the likely volume of ice-dammed lakes and the probable triggering water levels that lead to GLOFs

Deleted: (Zhang et al., 2023)

Deleted: a critical dep

Deleted: ice-dammed lakes

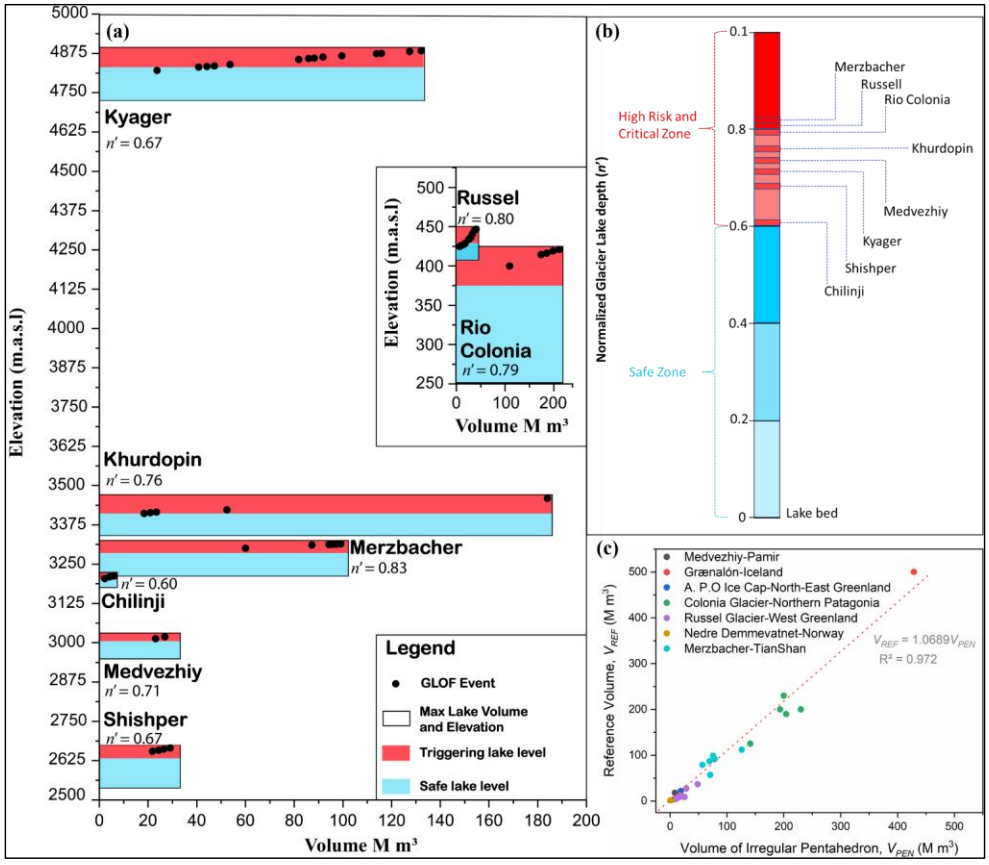

Figure 9: (a) The maximum volume of ice-dammed glacier lakes that result in GLOFs related to water surface elevation. In this representation, the red bands are defined by the range of *n'* values recorded just before each GLOF event was initiated. The blue band represents lakes with volumes below the normalized lake depth of 0.60. **(b)** Normalized critical lake depths and the high-risk and critical zones for GLOFs, with an inferred gradation for risk within the safe zone, are shown by shades of blue. **(c)** The relationship between the reference volume (V_{REF}) and the measured volume (V_{PEN}) was obtained through a geometric approach. The location of these glaciers is presented in Fig. S1.

Despite the absence of long-term records, those that are available indicate that glacial ice-dammed lakes worldwide exhibit consistent behavior in terms of lake formation, filling, and volume gain in response to low glacier velocity (Bazai et al., 2021).

Deleted: 8

Deleted: The maximum volume of ice-dammed glacier lakes that result in GLOFs related to elevation of the water surface. In this representation, the red bands are defined by the range of *n'* values recorded just before each GLOF event was initiated. The blue band represents lakes with volumes below the normalized lake depth of 0.60.**(b)** Normalized critical lake depths and the high-risk and critical zones for GLOFs, with an inferred gradation for risk within the safe zone are shown by shades of blue. **(c)** The relationship between the reference volume (V_{REF}) and the measured volume (V_{PEN}), the latter obtained through a geometric approach. The location of these glaciers are presented in Fig. S1

Additionally, specific water pressure and critical normalized lake depth values for initiating outburst floods are evident (Fig. 8).

Building upon the information presented in Figure 8 for the Karakoram, Figure 9, based on 50 GLOF events from ten glacial ice-dammed lakes, offers a depiction of the conditions under which glacier lake volume measurements are estimated with high accuracy. Considering lakes other than within the Karakoram, the lake elevation (Fig. 9a) at the time of a GLOF was available for five lakes that have triggered more than twice (Chilinji, Medvezhiy, Merzbacher, Russell, Rio Colonia)., enabling the calculation of the normalized lake depths (Fig. 9b). The data points in Fig. 9c represent 27 lakes within the Pamir, Tianshan, Greenland, and northern Patagonia, for which lake volume data are available in the literature. These latter data were used to establish a relationship between the lake volume estimated using Equation 2 and the reported volumes ($R^2 = 0.972$; Fig. 9c). Figures 9a and b serve as key components and summaries for this discussion, identifying the lake volumes, elevations, and the critical normalized depth values for GLOF outbursts. The measured lake volumes and the related water surface elevations are shown in Fig. 9a, together with critical depth values (*n'*). Critical normalized lake depth values (*n'*) exceed 0.60 in all cases of GLOFs (Fig. 9b). From this result, we infer that a safe lake level can be defined as ≤ 0.60, while the trigger level is ≥ 0.60. Values of *n'* < 0.60 were associated with slow, non-catastrophic lake drainage. Therefore, in the case of future ice-dammed lakes, values of critical depth (*n'*) exceeding 0.60 should be a cause for concern, and 0.60 would serve as a warning level. These findings suggest that future exploration should concentrate on specific volume and depth parameters to determine critical thresholds associated with normalized depth and the associated lake volume for future predictive purposes.

Estimating the volume of an undrained ice-dammed lake from a field survey is dangerous due to floating ice, rugged terrain, and sudden drawdowns. The utilization of DEM measurements for lake volume estimation may also introduce high uncertainties or errors due to the difficulty in defining the lake depths (Carrivick et al., 2020; Emmer, 2018). However, for rapid response or mitigation policy purposes, the empirical model (Equations 1 or 2) used in the current study proves to be quite efficient when applied to estimate the lake volume before a GLOF, not least because the errors in measurements from both satellite and UAV images are now quite small, as noted within the Method.

Although GLOFs cannot be predicted from this approach, the likely volume of water that might be released catastrophically can be determined. For sites that are deemed to pose a threat to human life and infrastructure, once the lake volume is better constrained, either through DEM analysis or geometric considerations, the value of *n'* for any specific lake provides a ready indicator of the probability of an imminent GLOF. In contrast to the lower trend for water pressures associated with the Kyager lakes, the higher water pressures required to cause the Khurdopin and Shishper lakes to empty may reflect greater structural integrity, possibly related to a greater downstream extent of the glacier dams. These structural issues can be examined in the future. Still, at this stage, if *n'* exceeds 0.6, an initial general warning could be issued to communities downstream of the ice dam. In principle, the estimated volume of a potential GLOF can then be routed downstream using standard hydrodynamic flood routing procedures to determine the timing, depth, and extent of flooding at locations where inundation is forecast. Thus, the severity of the likely impact on humankind can be determined, and specific warning times can be derived from the modelled rate of travel of the GLOFs. These results represent a step forward from the observations made by Carrivick et al. (2020), who

Deleted: Additionally, specific water pressure and critical normalized lake depth values for initiating outburst floods are evident (Fig. 7). Building upon the information presented in Figure 7 for the Karakoram, Figure 8, based on 50 GLOF events from ten glacial ice-dammed lakes, offers a depiction of the conditions under which glacier lake volume measurements are estimated with high accuracy. Considering lakes other than within the Karakoram, the lake depth (Fig. 8a) at the time of a GLOF was available for five lakes that have triggered more than twice (Chilinji, Medvezhiy, Merzbacher, Russell, Rio Colonia)., enabling the calculation of the normalized lake depth. The data points in Fig. 8c represent 27 lakes within the Pamir, Tianshan, Greenland, and northern Patagonia, for which volume data are available in the literature. These latter data were used to establish a relationship between the lake volume estimated using Equation 2 and the reported volumes ($R^2 = 0.986$; Fig. 8c).Additionally, specific water pressure and critical normalized lake depth values for initiating outburst floods are evident (Fig. 7). Building upon the information presented in Figure 7 for the Karakoram, Figure 8, based on 50 GLOF events from ten glacial ice-dammed lakes, offers a depiction of the conditions under which glacier lake volume measurements are estimated with high accuracy. Considering lakes other than within the Karakoram, the lake depth (Fig. 8a) at the time of a GLOF was available for five lakes that have triggered more than twice (Chilinji, Medvezhiy, Merzbacher, Russell, Rio Colonia)., enabling the calculation of the normalized lake depth. The data points in Fig. 8c represent 27 lakes within the Pamir, Tianshan, Greenland, and northern Patagonia, for which volume data are available in the literature. These latter data were used to establish a relationship between the lake volume estimated using Equation 2 and the reported volumes ($R^2 = 0.986$; Fig. 8c).¶ Figures 8a and b serve as key components and summaries for this discussion, identifying the lake volumes, elevations, and the critical normalized depth values for GLOF outbursts. The measured lake volumes and the related water surface elevations are shown in Fig. 8a, together with critical depth values (*n'*). Critical depth values (*n'*) exceed 0.60 in all cases of GLOFs (Fig. 8b). From this result, we infer that a safe lake level can be defined as ≤ 0.60, while the trigger level is ≥ 0.60. Values of *n'* < 0.60 were associated with slow, non-catastrophic lake drainage. Figures 8a and b serve as key components and summaries for this discussion, identifying the lak ...

Deleted: (Fig. 06b)

Deleted: Equations 1 or 2) used in the current study proves to be quite efficient when applied to estimate the lake volume before a GLOF, not least because the errors in measurements from both satellite and UAV images are now quite small, as noted within the Method

Deleted: Understanding glacier surges, lake formation, and the interactions between lakes and glaciers is crucial for advancing knowledge and developing empirical or numerical GLOF models in mountainous regions (Carrivick et al., 2020; Quincey and Luckman, 2014). In this study, the glacier and lake interactions and their relationship have been explored, and their effect on lake volume and draining processes has been examined. Glacier surge speed is routinely determined using remote-sensing imagery (Paul, 2015), as is lake surface area (Quincey and Luckman, 2014). Thus, remote sensing provides a means to develop images similar to Fig. 5 for specific locations around the globe where ice-dammed lakes form due to glacier surging. Although the data within Fig. 5 are scattered, a negative relationship between surge velocity and lake volume is strongly implied. Specifically, data points scatter around a median trend according to a theoretical -2 power function (Fig. 5). Clearly ...

proposed the exploration of the interaction between lake water and glaciers to understand the lake formation process and identify lake depth, level, and volume. Based on this understanding, empirical models can be generated to predict GLOFs in a timely manner.

6. Conclusion

The hazards associated with glacier lake outburst floods (GLOFs) in cryospheric regions are increasing worldwide in response to climate change, posing a significant threat to inhabitants in densely populated areas, particularly in the Himalayan Karakoram and Hindu Kush regions. Year after year, there is a rise in human casualties and losses to residences, infrastructure, the energy sector, and local and international trade. Despite the escalating hazard, the understanding of these hazards remains limited. It is imperative to determine the causes of these hazards, make timely predictions, and formulate new mitigation policies to minimize losses. Herein, it has been shown tentatively that glacier surge speed may correlate negatively with ice-dammed lake volumes such that glacier dynamics control lake volumes. Identifying the critical depths, lake volumes, and pressures of ice-dammed lakes worldwide associated with GLOFs has indicated that GLOFs may be imminent when the normalized depth (n') for lakes exceeds a critical value (n' = 0.60) with a typical water pressure on the dam face exceeding 510 kPa. Comparing published surveyed lake volumes with geometric volume estimates for 23 GLOF events from the Karakoram and 27 events from around the world, linear least-squares regression (R^2 0.972) demonstrated that geometric estimates can be robust in the absence of detailed field or remote-sensing surveys.

Deleted: risk

Deleted: Herein it has been shown tentatively that glacier surge speed may correlate negatively with ice-dammed lake volumes such that glacier dynamics control lake volumes Identifying the

Deleted: and pressuresof ice-dammed lakes worldwide associated with GLOFs have indicated that GLOFs may be imminent when the non-dimensional depth (n') for lakes exceeds a critical value (n' = 0.60) with a typical water pressure on the dam face exceeding 510 kPa.

Deleted: non-dimensional

Deleted: published

Deleted: volume

Deleted: least-squares regression (R^2 = 0.93

Deleted: to

Deleted: 95

Deleted: Future research should further investigate the range of n' values and the nature of ice-failure mechanisms connecting lake drawdown and GLOF

Competing interests

The authors declare no conflict of interest.

Acknowledgments

This study was supported by the Second Tibet Plateau Scientific Expedition and Research Program (STEP) (Grant No. 2019QZKK0906) and the National Natural Science Foundation of China（Grant no. 42350410445). Special thanks to the monitoring team of Gilgit-Baltistan Disaster Management Authority (GBDMA), Quaid-i-Azam University, and Karakoram International University for their support and data sharing, and thanks to the Special Research Assistant program of the Chinese Academy of Sciences.

Author Contributions

N.A.B. conceptualized and designed the study and methodology, generated and compiled field data, processed data visualization, and drafted the manuscript. P.A.C. contributed to conceptualization, methodology, interpretation, discussion, review, and editing. P.C. supervised funding acquisition and commented on the paper, and H.W. contributed to compiling the field data. N.A.B., G.T.Z., J.W, D.Z.L, and J.H contributed to remote sensing data analysis.

Supplementary Information

Supplementary information for this paper is available in supplementary material and at https://doi.org/10.1016/j.earscirev.2020.103432 and https://doi.org/10.1016/j.gloplacha.2021.103710.

References

Ali, S., Khan, G., Hassan, W. *et al.:* Assessment of glacier status and its controlling parameters from 1990 to 2018 of Hunza Basin, Western Karakorum. *Environ Sci Pollut Res* ,28, 63178–63190, 2021.

Ali, S., Khan, G., Hassan, W., Qureshi, J. A., and Bano, I.: Assessment of glacier status and its controlling parameters from 1990 to 2018 of Hunza Basin, Western Karakorum, Environ. Sci. Pollut. Res., 28, 63178-63190, 2021.

Bazai, N. A., Cui, P., Carling, P. A., Wang, H., Hassan, J., Liu, D., Zhang, G., and Jin, W.: Increasing glacial lake outburst flood hazard in response to surge glaciers in the Karakoram, ESRv, 212, 103432, 2021.

Bazai, N. A., Cui, P., Liu, D., Carling, P. A., Wang, H., Zhang, G., Li, Y., and Hassan, J.: Glacier surging controls glacier lake formation and outburst floods: The example of the Khurdopin Glacier, Karakoram, Glob. Planet. Change, 208, 103710, 2022.

Berthier, E. and Brun, F.: Karakoram geodetic glacier mass balances between 2008 and 2016: persistence of the anomaly and influence of a large rock avalanche on Siachen Glacier, J. Glaciol, 65, 494-507, 2019.

Bhambri, R., Bolch, T., Kawishwar, P., Dobhal, D., Srivastava, D., and Pratap, B.: Heterogeneity in glacier response in the upper Shyok valley, northeast Karakoram, The Cryosphere, 7, 1385-1398, 2013.

Bhambri, R., Hewitt, K., Kawishwar, P., Kumar, A., Verma, A., Tiwari, S., and Misra, A.: Ice-dams, outburst floods, and movement heterogeneity of glaciers, Karakoram, Glob. Planet. Change, 180, 100-116, 2019.

Björnsson, H.: Subglacial lakes and jökulhlaups in Iceland, Glob. Planet. Change, 35, 255-271, 2003.

Bolch, T., Pieczonka, T., and Benn, D.: Multi-decadal mass loss of glaciers in the Everest area (Nepal Himalaya) derived from stereo imagery, The Cryosphere, 5, 349-358, 2011.

Bolch, T., Pieczonka, T., Mukherjee, K., and Shea, J. M.: Brief communication: Glaciers in the Hunza catchment (Karakoram) have been nearly in balance since the 1970s, The Cryosphere, 11, 531-539, 2017.

Byers, A. C., Somos-Valenzuela, M., Shugar, D. H., McGrath, D., Chand, M. B., and Avtar, R.: Brief Communication: An Ice-Debris Avalanche in the Nupchu Valley, Kanchenjunga Conservation Area, Eastern Nepal, EGUsphere, 2023, 1-8, 2023.

Carling, P. A., Jonathan, P., and Su, T.: Fitting limit lines (envelope curves) to spreads of geoenvironmental data, Prog. Phys. Geogr.: Earth Environ., 46, 272-290, 2022.

Carrivick, J. L. and Tweed, F. S.: A global assessment of the societal impacts of glacier outburst floods, Glob. Planet. Change, 144, 1-16, 2016.

Carrivick, J. L., Tweed, F. S., Sutherland, J. L., and Mallalieu, J.: Toward numerical modeling of interactions between ice-marginal proglacial lakes and glaciers, Front. Earth Sci., 2020. 500, 2020.

Consortium, R.: Randolph glacier inventory–a dataset of global glacier outlines: Version 6.0: technical report, global land ice measurements from space, Colorado, USA, Digital Media, 2017. 2017.

Cook, S. J., Kougkoulos, I., Edwards, L. A., Dortch, J., and Hoffmann, D.: Glacier change and glacial lake outburst flood risk in the Bolivian Andes, The Cryosphere, 10, 2399-2413, 2016.

Copland, L., Sylvestre, T., Bishop, M. P., Shroder, J. F., Seong, Y. B., Owen, L. A., Bush, A., and Kamp, U.: Expanded and recently increased glacier surging in the Karakoram, Arct. Antarct. Alp. Res., 43, 503-516, 2011.

Cui, P., Chen, R., Xiang, L., and Su, F.: Risk analysis of mountain hazards in Tibetan plateau under global warming, Progressus Inquisitiones De Mutatione Climatis, 2, 103-109, 2014.

Cui, P., Su, F., Zou, Q., Chen, N., and Zhang, Y.: Risk assessment and disaster reduction strategies for mountainous and meteorological hazards in Tibetan Plateau, Chin. Sci. Bull., 60, 3067-3077, 2015.

Dehecq, A., Gourmelen, N., Gardner, A. S., Brun, F., Goldberg, D., Nienow, P. W., Berthier, E., Vincent, C., Wagnon, P., and Trouvé, E.: Twenty-first century glacier slowdown driven by mass loss in High Mountain Asia, Nat. Geosci., 12, 22-27, 2019.

Dillencourt, M. B., Samet, H., and Tamminen, M.: A general approach to connected-component labeling for arbitrary image representations, Journal of the ACM (JACM), 39, 253-280, 1992.

Emmer, A.: Glacier retreat and glacial lake outburst floods (GLOFs). In: Oxford Research Encyclopedia of Natural Hazard Science, 2017.

Emmer, A.: GLOFs in the WOS: Bibliometrics, geographies and global trends of research on glacial lake outburst floods (Web of Science, 1979–2016), NHESS, 18, 813, 2018.

Emmer, A. and Vilímek, V.: Lake and breach hazard assessment for moraine-dammed lakes: an example from the Cordillera Blanca (Peru), NHESS, 13, 1551-1565, 2013.

Entwistle, N. and Heritage, G.: An evaluation DEM accuracy acquired using a small unmanned aerial vehicle across a riverine environment, Int. j. new Technol. Res, 3, 43-48, 2017.

Entwistle, N. S. and Heritage, G. L.: Small unmanned aerial model accuracy for photogrammetrical fluvial bathymetric survey, J. Appl. Remote Sens., 13, 014523, 2019.

Deleted: ¶
¶

Farinotti, D., Immerzeel, W. W., de Kok, R. J., Quincey, D. J., and Dehecq, A.: Manifestations and mechanisms of the Karakoram glacier Anomaly, Nat. Geosci, 13, 8-16, 2020.
Frey, H., Machguth, H., Huss, M., Huggel, C., Bajracharya, S., Bolch, T., Kulkarni, A., Linsbauer, A., Salzmann, N., and Stoffel, M.: Estimating the volume of glaciers in the Himalayan–Karakoram region using different methods, The Cryosphere, 8, 2313-2333, 2014.
Gao, Y., Liang, P., Qi, M., Yao, X., Ma, X., Mu, J., and Li, L.: Topography and accumulation rate as controls of asynchronous surging behaviour in the eastern and western branches of the Western Kunlun Glacier, Northwestern Tibetan Plateau, Int. J. Digital Earth, 17, 2353112, 2024.
Gardelle, J., Berthier, E., and Arnaud, Y.: Slight mass gain of Karakoram glaciers in the early twenty-first century, Nat. Geosci, 5, 322-325, 2012.
Gardelle, J., Berthier, E., Arnaud, Y., and Kaab, A.: Region-wide glacier mass balances over the Pamir-Karakoram-Himalaya during 1999-2011 (vol 7, pg 1263, 2013), 2013. 2013.
Haeberli, W.: Frequency and characteristics of glacier floods in the Swiss Alps, Ann. Glaciol., 4, 85-90, 1983.
Haemmig, C., Huss, M., Keusen, H., Hess, J., Wegmüller, U., Ao, Z., and Kulubayi, W.: Hazard assessment of glacial lake outburst floods from Kyagar glacier, Karakoram mountains, China, Annals of Glaciology, 55, 34-44, 2014.
Harrison, S., Kargel, J. S., Huggel, C., Reynolds, J., Shugar, D. H., Betts, R. A., Glasser, N., Haritashya, U. K., Klimeš, J., and Reinhardt, L.: Climate change and the global pattern of moraine-dammed glacial lake outburst floods, TC, 12, 2018.
Hewitt, K.: Natural dams and outburst floods of the Karakoram Himalaya, IAHS, 138, 259-269, 1982.
Hewitt, K.: Recent glacier surges in the Karakoram Himalaya, south central Asia, Eos, 78, 46, 1998.
Hewitt, K. and Liu, J.: Ice-dammed lakes and outburst floods, Karakoram Himalaya: historical perspectives on emerging threats, Phys. Geogr., 31, 528-551, 2010.
Huggel, C., KääB, A., Haeberli, W., Teysseire, P., and Paul, F.: Remote sensing based assessment of hazards from glacier lake outbursts: a case study in the Swiss Alps, CaGeJ, 39, 316-330, 2002.
Jackson, M., Azam, M., Baral, P., Benestad, R., and Brun, F.: Consequences of climate change for the cryosphere in the Hindu Kush Himalaya, ICIMOD (P. Wester, S. Chaudhary, N. Chettri, M. Jackson, A. Maharjan, S. Nepal & JF Steiner [Eds.]), Water, ice, society, and ecosystems in the Hindu Kush Himalaya: An outlook, 2023. 17-71, 2023.
John, Clague, and, Stephen, and Evans: A review of catastrophic drainage of moraine-dammed lakes in British Columbia, QSRv, 2000. 2000.
Kääb, A. and Girod, L.: Brief communication: Rapid∼ 335× 10 6 m 3 bed erosion after detachment of the Sedongpu Glacier (Tibet), The Cryosphere, 17, 2533-2541, 2023.
Kääb, A., Treichler, D., Nuth, C., and Berthier, E.: Brief Communication: Contending estimates of 2003–2008 glacier mass balance over the Pamir–Karakoram–Himalaya, TC, 9, 2015.
Kreutzmann, H.: Habitat conditions and settlement processes in the Hindukush-Karakoram, Petermanns Geogr. Mitt, 138, 337-356, 1994.
Leprince, S., Avouac, J.-P., and Ayoub, F.: Ortho-rectification, coregistration, and subpixel correlation of optical satellite and aerial images. Google Patents, 2012.
Leprince, S., Barbot, S., Ayoub, F., and Avouac, J.-P.: Automatic and precise orthorectification, coregistration, and subpixel correlation of satellite images, application to ground deformation measurements, ITGRS, 45, 1529-1558, 2007.
Li, Y., Cui, Y., Hu, X., Lu, Z., Guo, J., Wang, Y., Wang, H., Wang, S., and Zhou, X.: Glacier retreat in Eastern Himalaya drives catastrophic glacier hazard chain, Geophys. Res. Lett., 51, e2024GL108202, 2024.
Mason, K.: Indus floods and Shyok glaciers, Himal. J, 1, 10-29, 1929.
McFeeters, S. K.: The use of the Normalized Difference Water Index (NDWI) in the delineation of open water features, Int. J. Remote Sens., 17, 1425-1432, 1996.
Minora, U., Bocchiola, D., D'Agata, C., Maragno, D., Mayer, C., Lambrecht, A., Mosconi, B., Vuillermoz, E., Senese, A., and Compostella, C.: 2001–2010 glacier changes in the Central Karakoram National Park: a contribution to evaluate the magnitude and rate of the" Karakoram anomaly", The Cryosphere Discussions, 7, 2891-2941, 2013.
Mu, J., Gao, Y., and Liang, P.: Hydrological control of the surging behaviour of the Ghujerab River Head Glacier, Karakoram (2019–2023): Insights from high-temporal-resolution remote sensing monitoring, J. Hydrol.: Reg. Stud., 53, 101768, 2024.
Neupane, R., Chen, H., and Cao, C.: Review of moraine dam failure mechanism, Geomatics Nat. Hazards Risk, 10, 1948-1966, 2019.
Ng, F.: Climatic control on the peak discharge of glacier outburst floods, Geophys. Res. Lett., 2007. 2007.
Paul, F.: Revealing glacier flow and surge dynamics from animated satellite image sequences: examples from the Karakoram, The Cryosphere, 9, 2201-2214, 2015.
Quincey, D. and Luckman, A.: Brief Communication: On the magnitude and frequency of Khurdopin glacier surge events, The Cryosphere, 8, 571-574, 2014.
Rea, B. R. and Evans, D. J.: An assessment of surge-induced crevassing and the formation of crevasse squeeze ridges, J. Geophys. Res.: Earth Surf., 116, 2011.
Richardson, S. D. and Reynolds, J. M.: An overview of glacial hazards in the Himalayas, Quat Int, 65, 31-47, 2000.

Rick, B., McGrath, D., McCoy, S., and Armstrong, W.: Unchanged frequency and decreasing magnitude of outbursts from ice-dammed lakes in Alaska, Nat. Commun., 14, 6138, 2023.
Rodriguez, E., Morris, C. S., and Belz, J. E.: A global assessment of the SRTM performance, Photogrammetric Engineering & Remote Sensing, 72, 249-260, 2006.
Round, V., Leinss, S., Huss, M., Haemmig, C., and Hajnsek, I.: Surge dynamics and lake outbursts of Kyagar Glacier, Karakoram, TC, 11, 723-739, 2017.
Sattar, A., Goswami, A., Kulkarni, A. V., and Das, P.: Glacier-surface velocity derived ice volume and retreat assessment in the dhauliganga basin, central himalaya–A remote sensing and modeling based approach, Front. Earth Sci., 7, 105, 2019.
Shangguan, D., Ding, Y., Liu, S., Xie, Z., Pieczonka, T., Xu, J., and Moldobekov, B.: Quick release of internal water storage in a glacier leads to underestimation of the hazard potential of glacial lake outburst floods from lake merzbacher in central tian shan mountains, Geophys. Res. Lett., 44, 9786-9795, 2017.
Shangguan, D., Liu, S., Ding, Y., Guo, W., Xu, B., Xu, J., and Jiang, Z.: Characterizing the May 2015 Karayaylak Glacier surge in the eastern Pamir Plateau using remote sensing, JGlac, 62, 944-953, 2016.
Sharp, M.: "Crevasse-fill" ridges—a landform type characteristic of surging glaciers?, Geogr. Ann. Ser. A Phys. Geogr., 67, 213-220, 1985.
Shrestha, F., Steiner, J. F., Shrestha, R., Dhungel, Y., Joshi, S. P., Inglis, S., Ashraf, A., Wali, S., Walizada, K. M., and Zhang, T.: A comprehensive and version-controlled database of glacial lake outburst floods in High Mountain Asia, Earth Syst. Sci. Data, 15, 3941-3961, 2023.
Singh, H., Varade, D., de Vries, M. V. W., Adhikari, K., Rawat, M., Awasthi, S., and Rawat, D.: Assessment of potential present and future glacial lake outburst flood hazard in the Hunza valley: A case study of Shisper and Mochowar glacier, Sci. Total Environ., 868, 161717, 2023.
Steiner, J. F., Kraaijenbrink, P. D., Jiduc, S. G., and Immerzeel, W. W.: Brief communication: The Khurdopin glacier surge revisited-Extreme flow velocities and formation of a dammed lake in 2017, TC, 12, 95-101, 2018.
Stuart-Smith, R., Roe, G., Li, S., and Allen, M.: Increased outburst flood hazard from Lake Palcacocha due to human-induced glacier retreat, Nat. Geosci., 14, 85-90, 2021.
Tonkin, T. N. and Midgley, N. G.: Ground-control networks for image based surface reconstruction: An investigation of optimum survey designs using UAV derived imagery and structure-from-motion photogrammetry, Remote Sens, 8, 786, 2016.
Trabant, D. C., March, R., and Thomas, D.: Hubbard Glacier, Alaska: Growing and advancing in spite of global climate change and the 1986 and 2002 Russell Lake outburst floods, US Geological Survey, 907, 786-7100, 2003.
Vandekerkhove, E.: Impact of climate change on the occurrence of late Holocene glacial lake outburst floods in Patagonia: A sediment perspective, 2021. Ghent University, 2021.
Veh, G., Lützow, N., Kharlamova, V., Petrakov, D., Hugonnet, R., and Korup, O.: Trends, breaks, and biases in the frequency of reported glacier lake outburst floods, Earth's Future, 10, e2021EF002426, 2022.
Veh, G., Lützow, N., Tamm, J., Luna, L. V., Hugonnet, R., Vogel, K., Geertsema, M., Clague, J. J., and Korup, O.: Less extreme and earlier outbursts of ice-dammed lakes since 1900, Nature, 614, 701-707, 2023.
Werder, M. A., Bauder, A., Funk, M., and Keusen, H. R.: Hazard assessment investigations in connection with the formation of a lake on the tongue of Unterer Grindelwaldgletscher, Bernese Alps, Switzerland, NHESS, 10, 474-479 Vol. 471, 2010.
Xu, M., Bogen, J., Wang, Z., Bønsnes, T. E., and Gytri, S.: Pro-glacial lake sedimentation from jökulhlaups (GLOF), Blåmannsisen, northern Norway, ESPL, 40, 654-665, 2015.
Yao, T., Thompson, L. G., Mosbrugger, V., Zhang, F., Ma, Y., Luo, T., Xu, B., Yang, X., Joswiak, D. R., and Wang, W.: Third pole environment (TPE), Environ. Dev., 3, 52-64, 2012.
Yao, X., Liu, S., and Wei, J.: Reservoir capacity calculation and variation of Moraine-dammed Lakes in the North Himalayas: a case study of Longbasaba Lake, Aata Geographica Sinica, 65, 1381-1390, 2010.
Yong, Nie, Yongwei, Sheng, Qiao, Liu, Linshan, Liu, Shiyin, and Liu: A regional-scale assessment of Himalayan glacial lake changes using satellite observations from 1990 to 2015, Remote Sens. Environ., 2017. 2017.
You, C. and Xu, C.: Himalayan glaciers threatened by frequent wildfires, Nat. Geosci., 15, 956-957, 2022.
Zhang, G., Bolch, T., Yao, T., Rounce, D. R., Chen, W., Veh, G., King, O., Allen, S. K., Wang, M., and Wang, W.: Underestimated mass loss from lake-terminating glaciers in the greater Himalaya, Nat. Geosci., 16, 333-338, 2023.
Zhang, T., Li, D., East, A. E., Walling, D. E., Lane, S., Overeem, I., Beylich, A. A., Koppes, M., and Lu, X.: Warming-driven erosion and sediment transport in cold regions, Nature Reviews Earth & Environment, 3, 832-851, 2022.
Zhang, X. S., Zhou, Y.C., et al.,: The Researches Of Glacier Lake Outburst Floods Of The Yarkant River In Xinjiang, Sci. China, Ser. B: Chem., 1990. 120-130+132, 1990.
Zhao, T.-y., Yang, M.-y., Walling, D. E., Zhang, F.-b., and Zhang, J.-q.: Using check dam deposits to investigate recent changes in sediment yield in the Loess Plateau, China, Global Planet. Change, 152, 88-98, 2017.
Zheng, G., Allen, S. K., Bao, A., Ballesteros-Cánovas, J. A., Huss, M., Zhang, G., Li, J., Yuan, Y., Jiang, L., and Yu, T.: Increasing risk of glacial lake outburst floods from future Third Pole deglaciation, Nat. Clim. Change, 11, 411-417, 2021.

Zhu, Y., Liu, S., Brock, B. W., Tian, L., Yi, Y., Xie, F., Shangguan, D., and Shen, Y.: Debris cover effects on energy and mass balance of Batura Glacier in the Karakoram over the past 20 years, Hydrol. Earth Syst. Sci., 28, 2023–2045, 2024.